Aus der

Universitätsklinik für Kinder- und Jugendmedizin Tübingen

Abteilung Kinderheilkunde I mit Poliklinik

Hämatologie, Onkologie, Gastroenterologie,
Nephrologie, Rheumatologie

Design and application of prime editing to target ARSA P426L mutation in a metachromatic leukodystrophy patient

Inaugural-Dissertation
zur Erlangung des Doktorgrades
der Medizin

der Medizinischen Fakultät
der Eberhard Karls Universität
zu Tübingen

vorgelegt von

Trosien, Paul Luis

2026

Dekanin:	Professorin Dr. S. Y. Brucker
1. Berichterstatter:	Professor Dr. Dr. M. Mezger
2. Berichterstatter:	Professorin Dr. E. Reisinger

Tag der Disputation: 02.07.2026

This thesis is dedicated to my parents Beate & Joachim

for their unconditional support, sacrifices and love.

Index

List of figures

List of tables

List of abbreviations

A:	Adenine
AAV:	Adeno-associated virus
allo-HSCT:	Allogeneic hematopoietic stem cell transplantation
ARSA:	Arylsulfatase A (written *ARSA* when referring to the gene, written ARSA when meaning the enzyme)
ARCA:	Anti-Reverse Cap Analog
BBB:	Blood-brain barrier
bp:	Base pair
C:	Cytosine
CNS:	Central nervous system
CRISPR-Cas9:	Clustered regularly interspaced short palindromic repeat - CRISPR associated protein 9
DSB:	Double Strand Break
DNA:	Deoxyribonucleic acid
EMA:	European Medicines Agency
ERT:	Enzyme replacement therapy
EJ:	Early juvenile (form of MLD)
EP:	Electroporation
Eppi:	Eppendorf tube
epegRNA:	engineered pegRNA
FACS:	Fluorescence activated cell sorting
FBS:	Fetal Bovine Serum
FDA:	Food and Drug Administration (U.S.)
G:	Guanine
GFP:	Green fluorescent protein
GvHD:	Graft-versus-Host-Disease
HDR:	Homology directed repair
HSPC:	Hematopoietic stem and progenitor cell
IL2RG:	Interleukin 2 Receptor Subunit Gamma
IT:	Intrathecal
IV:	Intravenous

IVT:	In vitro transcription
LB:	Lysogeny broth
Leu:	Leucine
LSD:	Lysosomal storage disease
LNPs:	Lipid nanoparticles
LV:	Lentivirus / lentiviral
LI:	Late infantile (form of MLD)
LJ:	Late juvenile (form of MLD)
MLD:	Metachromatic Leukodystrophy
MM:	Master Mix
MMR:	Mismatch repair
mRNA:	Messenger RNA
MSCs:	mesenchymal stromal cells
m-MLV:	Moloney Murine Leukemia Virus
NHEJ:	Non-homologous end joining
NSAIDs:	non-steroidal anti-inflammatory drugs
PCR:	Polymerase chain reaction
PBS:	Phosphate-buffered saline
Pro:	Proline
PNS:	Peripheral nervous system
PE:	Prime editor (PE1, PE2, PE3, PE4, PE5, PEmax etc.)
PSAP:	Prosaposin
P/S:	Penicillin/Streptomycin
pegRNA:	Prime editing guide RNA
RNA:	Ribonucleic acid
RT:	Reverse transcriptase
sgRNA:	Single guide RNA
ssRNA:	single-stranded RNA
T:	Thymine

1. Introduction

1.1 Metachromatic Leukodystrophy

Metachromatic Leukodystrophy (MLD) is a rare inherited lysosomal storage disease (LSD) affecting 1 in 40,000 to 160,000 individuals. It is primarily caused by mutations in the *Arylsulfatase A* (*ARSA*) gene, and less frequently in the P*rosaposin* (*PSAP*) gene (Cesani et al., 2016). These mutations lead to an actual or functional deficiency of the ARSA enzyme, which is crucial for metabolizing sulfatides in the central and peripheral nervous system (CNS & PNS) (Jonckheere et al., 2023). The resulting accumulation of sulfatides causes progressive demyelination and neurodegeneration. MLD patients exhibit a diverse range of symptoms that vary according to the specific form of the disease. Commonly observed symptoms include behavioral changes, cognitive decline, developmental delays, gradual loss of motor function, peripheral neuropathy as well as muscle weakness and stiffness (Fumagalli et al., 2021). In the early stages of MLD, not all symptoms are typically present, as the disease follows a progressive course that ultimately results in the patient's death (van Rappard et al., 2015).

MLD can be classified into different forms based on the age of onset, symptom progression, and the rate at which the disease advances. This classification includes the late infantile form (LI) with an age of onset < 2,5 years, early juvenile form (EJ) with an age of onset from 2,6 - 6 years, late juvenile form (LJ) with an age of onset from 6 - 16 years and adult form with age of onset ≥16 years (Jonckheere et al., 2023). The course of the disease varies significantly based on the form. While LI and EJ forms are characterized by rapid disease progression, LJ and adult forms typically have a milder disease course with slow progression over time. Certain conclusions about the clinical course can be drawn from the genotype. While mutations with no residual ARSA enzyme activity are linked to the LI form, mutations with some residual ARSA activity are linked to the late onset forms (Jonckheere et al., 2023).

Also there seems to be a specific genotype-phenotype correlation for the late onset forms but not for the LI form (Rauschka et al., 2006). At disease onset,

patients homozygous for the *ARSA* P426L mutation displayed progressive motor and sensory deficits, while patients homozygous for *ARSA* 1179S mutation exhibited mental disturbance but showed little to no impairment of motor function. However as the disease progresses, these differences vanish and symptoms converge (Rauschka et al., 2006)

To conclude, all forms of MLD result in significant functional impairment and profoundly diminish the quality of life of the patient (Fumagalli et al., 2021).

1.2 Treatment approaches

Treatment options for MLD are currently limited and predominantly non-curative. However, extensive ongoing research and the development of new technologies raise hope to find a potential cure in the future.

1.2.1 Allogeneic Hematopoietic stem cell transplantation

For a long time, allogeneic hematopoietic stem cell transplantation (allo-HSCT) has been the only available treatment for MLD (Peters & Steward, 2003). This method is based on transplanting hematopoietic stem and progenitor cells (HSPCs) from a suitable donor to the patient, and leads to engraftment of donor-derived microglial cells in the patient's CNS. This results in an increase of ARSA enzyme levels in the CNS, slowing or halting demyelination and can even lead to remyelination (Groeschel et al., 2016). The exact mechanisms that mediate these effects will be discussed in chapter **1.2.5** of this work. The efficacy of allo-HSCT varies widely depending on the form and stage of the disease (Jonckheere et al., 2023). Studies suggest a clear advantage for patients suffering from the juvenile forms, with the level of success depending on various disease parameters at the time of allo-HSCT (van Rappard et al., 2016). Moreover patients with the adult form seem to benefit from allo-HSCT under specific circumstances (Videbæk et al., 2021). For the late infantile form unfortunately there is no advantage compared to the natural course of the disease, regardless of the presence or absence of symptoms at the start of the treatment (Boucher et al., 2015). This could possibly be explained by the long time needed for engraftment after allo-HSCT, which is approximately 100 days (van den Broek et al., 2018). This, together with the lack of a newborn

screening for MLD, makes allo-HSCT an unsuitable treatment option for patients suffering from the LI form. The outcome for the other forms depends on the level of symptoms at the beginning of the therapy. Therefore, not all patients will profit in the same way from allo-HSCT. Furthermore, allo-HSCT only affects the CNS while the PNS manifestations of MLD remain unchanged by this treatment approach. (Beerepoot et al., 2019; Beschle et al., 2020; Boucher et al., 2015)

1.2.2 Enzyme replacement therapy (ERT)

ERT is based on the infusion of human ARSA enzyme to supplement the low or absent production in MLD patients. With the exact therapeutic mechanism still being a topic of research (Jonckheere et al., 2023), it was shown in mice that repeated administration of ARSA enzyme, by intravenous (IV) or intrathecal (IT) route, led to significant reduction in sulfatide deposits (Stroobants et al., 2011), reduction of pathological changes in the CNS and amelioration of associated symptoms (Matthes et al., 2012; Matzner et al., 2009). This led to clinical trials testing IV and IT enzyme replacement in human MLD patients (NCT00633139, NCT01510028). Unfortunately, in the IV trial it was not possible to alter the course of the disease significantly (Í Dali et al., 2021), probably caused by ARSA crossing the blood-brain-barrier in insufficient quantities (Groeschel et al., 2016). Similarly, the results of the IT trial showed underwhelming effects in slowing disease progression among patients (Í Dali et al., 2020). Another clinical trial with a higher dose of IT administered enzyme is ongoing (NTC03771898) and results have to be evaluated in the future to draw conclusions about the potential value of ERT in the treatment of MLD. In contrast to allo-HSCT, ERT is expected to cause benefits also in the PNS, as IT administered enzyme could also enter the systemic circulation via reabsorption of cerebrospinal fluid (CSF) (Jonckheere et al., 2023). One downside however is the need for frequent administration due to low half life of the enzyme in the CSF (Stroobants et al., 2011). Depending on the results of ongoing trials, ERT could potentially be a valuable part of a multimodal therapy concept for MLD in the future (Jonckheere et al., 2023), yet ERT alone has its limitations.

1.2.3 Libmeldy

Libmeldy is a gene therapy based on the transplantation of autologous HSPCs which are ex-vivo transduced with healthy *ARSA* gene via a lentiviral (LV) vector. This procedure leads to supra-physiological ARSA production within the transduced cells (500-1000%) due to an overexpression caused by a stronger promoter (Jonckheere et al., 2023). The transplanted cells then cross the blood-brain barrier, differentiate into microglia and produce functional ARSA enzyme at the site of pathology (Messina & Gissen, 2023). The exact mechanisms of action will again be discussed in chapter **1.2.5**. After successful experiments in ARSA deficient mice (Biffi et al., 2006; Biffi et al., 2004; Matzner et al., 2002), clinical trials with human MLD patients were started (NCT01560182, NCT03392987, NCT04283227). Results published from NCT01560182 were promising as most of the treated patients showed normal motor and cognitive development as well as prevention or delay of central and peripheral demyelination and brain atrophy. Also, no abnormal clonal proliferation or replication-competent LV was observed (Fumagalli et al., 2022). As a result, Libmeldy was approved by the EMA (European Medicines Agency) for the treatment of non-symptomatic LI form and non- and early-symptomatic EJ forms[1] and approval by the FDA (U.S. Food and Drug Administration) is expected to be granted soon. Long term surveillance and further studies will shed light to the theoretical risk of insertional mutagenesis with the possible induction of leukemia (Antony et al., 2022). Further investigation will be needed, to tell if this treatment will prove efficient also for the late onset forms of MLD.

1.2.4 Others

It seems that neuroinflammation plays an important role in the pathomechanism of MLD (Jonckheere et al., 2023). Therefore, modulating the immune response against accumulated sulfatides could also be part of a multimodal therapy approach for MLD in the future. For a variety of other LSDs, positive effects were observed for the use of nonsteroidal anti-inflammatory drugs (NSAIDs) in mice (Jeyakumar et al., 2004; Luzi et al., 2009; Smith et al., 2009). More

[1] https://www.ema.europa.eu/en/medicines/human/EPAR/libmeldy

research has to be done before we can evaluate the importance of immunomodulation specifically for treating MLD.

1.2.5 Therapy mechanisms

The way in which stem cell therapies like Libmeldy and allo-HSCT exert their therapeutic effects inside the patient's body is yet to be completely understood. Formerly, cross-correction was postulated to mediate the positive effects of HSCT (Antony et al., 2022). The cross-correction theory is based on the assumption that ARSA competent donor cells migrate to the brain, differentiate into microglia and secrete functional ARSA enzyme, which is then taken up by local cells, thereby „cross-correcting" the enzyme deficiency in these cells (Krägeloh-Mann & Groeschel, 2016). However, ARSA secreted by macrophages lacks mannose-6-phosphate, which is needed for the mannose-6-phosphate receptor-dependent endocytosis by the local cells (Muschol et al., 2002). Fittingly, a recent study found no evidence of enzymatic cross-correction in local astrocytes and oligodendrocytes after HSCT, while ARSA competent donor microglia were detected in abundance (Wolf et al., 2020). The authors suggest that the effect is rather caused by expression of anti-inflammatory markers and digestion of accumulated sulfatides by donor cells, acting as neuroprotective factor for resident oligodendrocytes, thereby enabling remyelination (Wolf et al., 2020). This emphasizes the potential value of immunomodulation in a future multimodal therapy approach for MLD (Wolf et al., 2020).

1.3 *ARSA* P426L mutation

ARSA P426L mutation is one of the two most frequently observed MLD causing mutations in Europe. Pro (Proline) to Leu (Leucine) substitution at the 426th amino acid of ARSA enzyme is caused by a C (Cytosine) to T (Thymine) transition at nucleotide 2381 of the *ARSA* gene. The resulting enzyme presents enzymatic activity but decreased stability, caused by defective oligomerization, which leads to rapid degradation. P426L mutation is mainly found in patients presenting with the adult or juvenile forms but can also rarely be found in late infantile MLD. (Lugowska et al., 2005)

1.4 Prime Editing and CRISPR-Cas9

The discovery and publication of the CRISPR-Cas9 (Clustered regularly interspaced short palindromic repeat - CRISPR associated protein 9) system in 2012 (Jinek et al., 2012) has led to significant progress on the field of gene therapy. For a lot of currently incurable diseases that are caused by specific genetic mutations, a curative gene therapeutic intervention now comes within reach (Mollanoori & Teimourian, 2018).

1.4.1 CRISPR-Cas9

The CRISPR-Cas9 system is comprised of a double-stranded breaks (DSBs) - inducing Cas9 endonuclease coupled to a single guide RNA (sgRNA), which guides the Cas9 protein to the desired cleavage site (Jinek et al., 2012). These double-stranded breaks are then repaired by the cell's innate repair mechanisms, non-homologous end joining (NHEJ) and homology directed repair (HDR) (**Figure 1**) (Kantor et al., 2020).

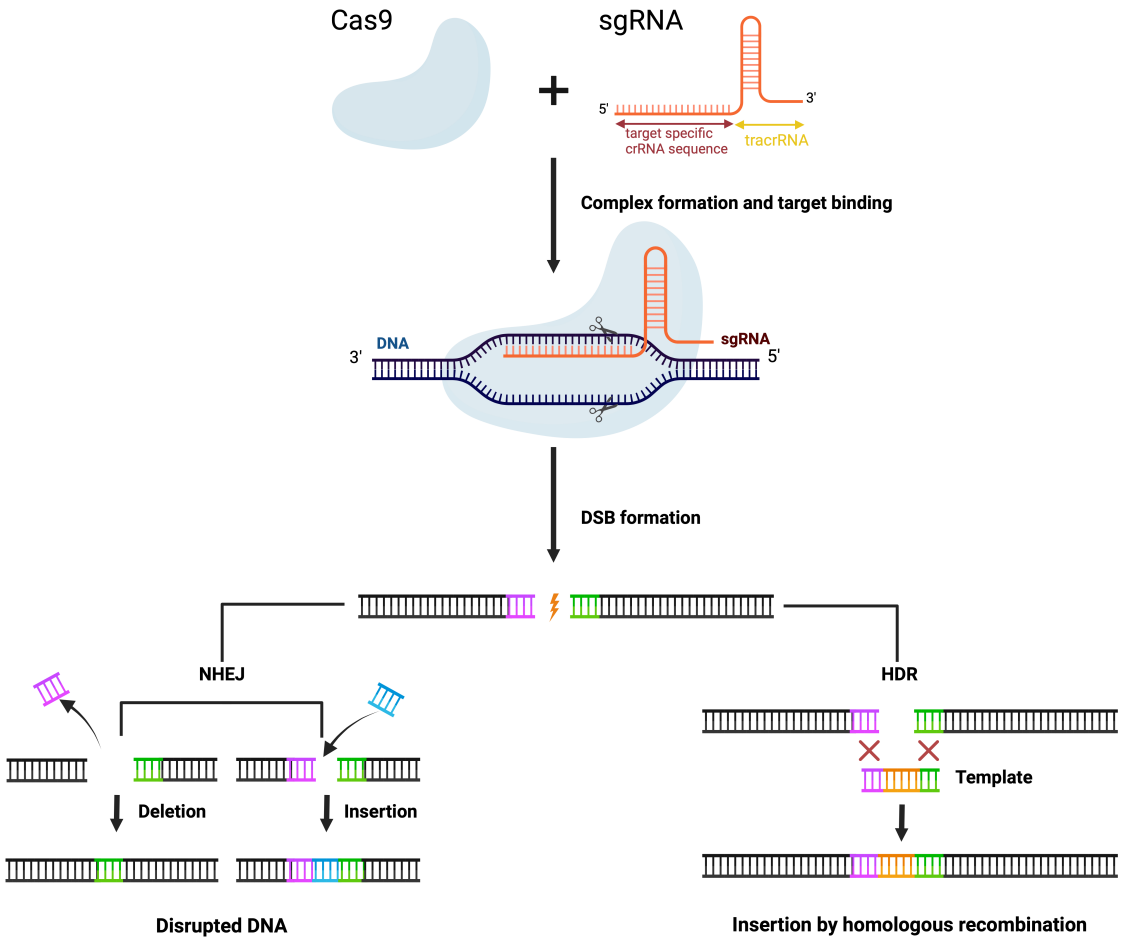

Figure 1 Scheme of CRISPR-Cas9 mechanism (Created with BioRender)

In case of NHEJ, the gene gets disrupted due to short insertions and deletions (indels). For the HDR pathway, it is possible to provide a repair template for the mechanism to integrate a desired sequence of nucleotides into the location of the DSB. In human cells, NHEJ is the dominant pathway to repair DSBs while HDR is restricted to dividing cells only, as it can only happen in S or G2 phase of the cell cycle (Li et al., 2019).

In a recent study, Antony et al. tried to integrate functional *ARSA* gene with the help of CRISPR-Cas9 and an AAV (Adeno-associated virus) delivered template into the genome of HSPCs. The authors achieved efficient integration of the transgene, although the results also showed significant indel formation and reduced cell recovery (Antony et al., 2022). The decline in cellular recovery was thought to arise from induction of p53 pathway caused by the DSBs and could potentially be a problem for successful host engraftment in patients after

transplantation (Antony et al., 2022). According to other publications, induction of p53 pathway in HSPCs often leads to apoptosis (Ihry et al., 2018). While Antony et al. showed that the ARSA activity in edited HSPCs increased (Antony et al., 2022), the formation of indels poses the risk of shifting the reading frame which could lead to inefficient transgene expression or an altered gene product exhibiting absent or impaired function.

To conclude, the CRISPR-Cas9 mechanism is very efficient in knock out (Dalvie et al., 2022) approaches disrupting a specific gene, but its capabilities to create a desired change or insert a functional gene are limited (Anzalone et al., 2019).

1.4.2 Prime Editing

Prime Editing is one step further in the evolution of CRISPR-Cas9, enabling precisely targeted editing of small stretches of nucleotides and single basepairs (Anzalone et al., 2019). This makes it an interesting tool to target disease-causing point mutations. Prime Editors consist of a Cas9 nickase (a catalytically impaired Cas9 endonuclease that induces single strand breaks called nicks instead of DSBs), fused to a reverse transcriptase (RT). To find and edit the target, a prime editing guide RNA (pegRNA) is needed (Anzalone et al., 2019). A pegRNA contains a guide sequence, which is complementary to the targeted region in the genome, as well as a template for the RT containing the desired edit and a primer binding site, which serves as starting point for the RT. (Anzalone et al., 2019)

The pegRNA guides the prime editing complex to its target site and, with one end, binds to the deoxyribonucleic acid (DNA) strand in which no edit should take place. The Cas9 nickase then nicks the opposite strand, where the edit should take place. After that, the RT synthesizes a new stretch of DNA containing the desired edit, which is subsequently incorporated into the DNA strand. The flap containing the original sequence is removed (Anzalone et al., 2019). The cells' innate DNA mismatch repair (MMR) mechanism then uses either the edited or the unedited strand as a template, thereby introducing a complementary edit into the unedited strand or removing the edit completely. (Anzalone et al., 2019)

A schematic overview of the prime editing mechanism is shown in **Figure 2.**

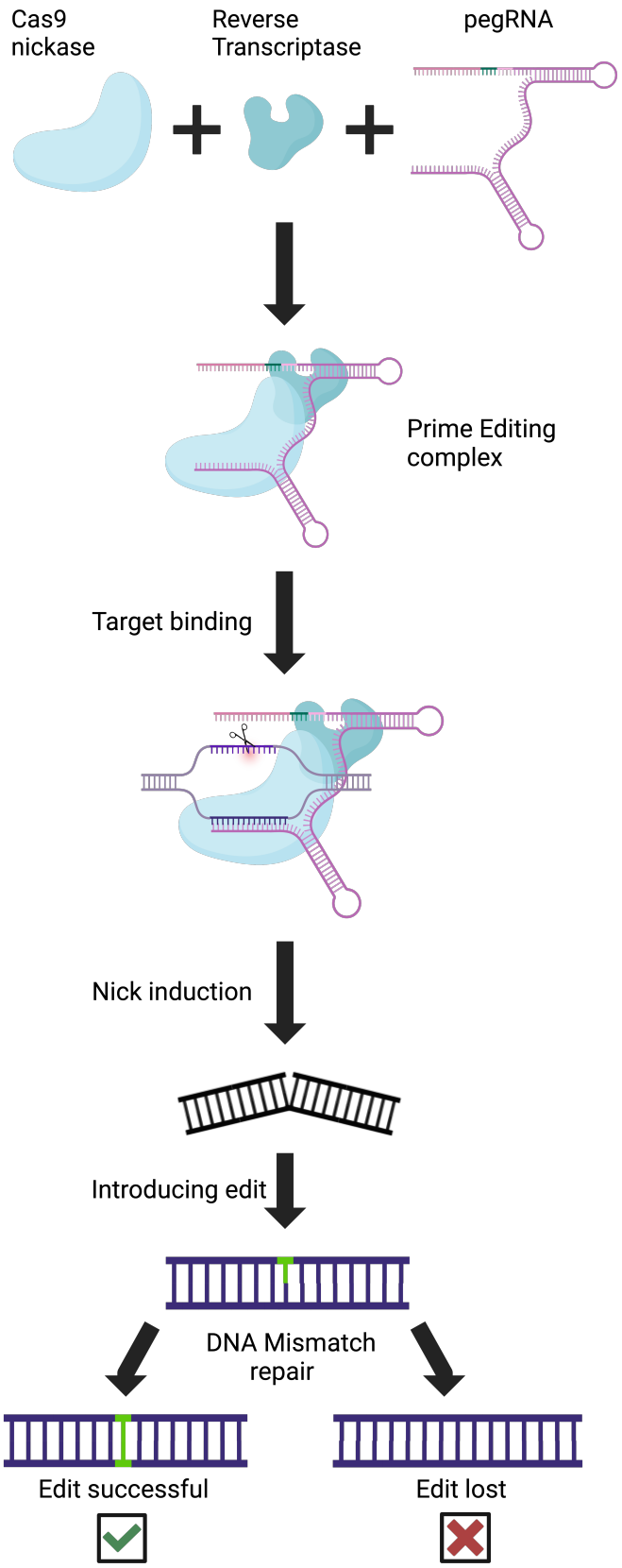

Figure 2 Scheme of Prime Editing mechanism (PE1 for simplicity) (Created with BioRender)

There are different evolutions of prime editors. Prime editor 1 (**PE1**) consists of a wild-type Moloney Murine Leukemia Virus (M-MLV) reverse transcriptase linked to a Cas9 nickase. For prime editor 2 (**PE2**), five amino acid substitutions were incorporated into the reverse transcriptase for enhanced DNA-RNA affinity, thermostability and enzyme processivity. For prime editor 3 (**PE3**), PE2 was supplemented with an additional single guide RNA (sgRNA), complementary to the edited sequence, but not the original one. This sgRNA directs the Cas9 nickase to nick the unedited strand, which is then repaired by the cell's innate repair mechanisms using the edited strand as a template, thereby solidifying the the edit and preventing removal of the edit by DNA mismatch repair. (Anzalone et al., 2019)

There are a couple of further modified prime editors like PE4, PE5, twin prime editing and PEmax systems which will not be discussed in this section as they were not utilized in the project (Anzalone et al., 2022; Chen et al., 2021).

1.4.3 Best tool to target ARSA P426L

CRISPR-Cas9 is very effective as a tool to knock out genes (Dalvie et al., 2022) but lacks the precision needed to edit one specific base. Therefore it is not suitable for our project. Prime editing can induce desired genomic changes like insertions, deletions and substitutions within the range of one to several bases with high precision. Base editing, another precision gene editing tool, provides more efficient editing than prime editing, but is limited by frequently altering nearby similar bases (Kantor et al., 2020). With the wild type locus of our target site corresponding to the fifth cytosine in a consecutive stretch, we chose prime editing over base editing to avoid unintended editing of nearby cytosine bases (Kantor et al., 2020).

1.4.4 Prime Editors used in the project

PE2 mechanism was used in the first transfections of K562 cells as it was already established in our research group (Hou et al., 2022). In the course of the project we switched to **PE3** due to achieving higher editing efficiency in our experiments.

1.5 Transfection by electroporation

There are different reported ways to effectively deliver the components used for genome editing and other gene therapeutic interventions into target cells. Electroporation (EP) (Schene et al., 2020; Zhao et al., 2006), Lipofection (Ejeskär et al., 2006) and delivery by LNPs (lipid nanoparticles) (Del Pozo-Rodríguez et al., 2016) are among the most effective methods for transfection. Because of the combination of good viability and transfection efficiency for various cell types and the preexisting expertise in our research group (Hou et al., 2022; Ureña-Bailén et al., 2022), we chose electroporation for this project.

1.6 Aim of the project

The goal of this project was to explore prime editing as a method to target the *ARSA* P426L locus in K562 cells as well as in HSPCs. An approach that would lead to successful correction of *ARSA* P426L in patient derived HSPCs could pave the way for a new gene therapeutic approach to treat MLD. Genetically corrected cells could be infused back to the patient in order to establish engraftment of ARSA competent HSPCs. Using patient derived cells would avoid the need to find a suitable donor, contrary to allo-HSCT. Precise editing of the mutated locus would diminish the potential risk of insertional mutagenesis posed by Libmeldy (Antony et al., 2022). Also, restoration of wild type *ARSA* sequence would lead to physiological levels of gene expression in genetically corrected HSPCs, avoiding potential side effects associated with supra-physiological gene expression.

The primary experimental strategy for this project was planned as follows:

1. Induction of P426L mutation in K562 cells
2. Induction of P426L mutation in healthy HSPCs
3. Correction of P426L mutation in MLD patient derived HSPCs

In addition to the *ARSA* P426L mutation, *IL2RG* c.458T>C mutation was targeted as a proof of concept. Inducing *IL2RG* c.458T>C mutation in K562 cells with prime editing has already been successfully demonstrated in prior studies, validating its feasibility as a target (Hou et al., 2022).

2. Materials and Methods

2.1 Ethical Approval

This project was approved by the Ethics Committee of the medical faculty of the Eberhard-Karls-Universität Tübingen under the reference number *0882018B01.*

2.2 Materials

2.2.1 Laboratory Equipment

Table 1 List of laboratory equipment

Article	**Manufacturer**
Centrifuges	Hettich, Rotixa 50 RS Eppendorf, Centrifuge 5430 R Hettich, Rotina 420R Benchmark, myFuge mini Biozym neoLab
Multi Block Heater	LAB-LINE, Multi-Blok Heater
NanoDrop 2000	Thermo scientific
PCR-Cyclers	BioRad, C1000 Touch
Pipettes	Eppendorf, research Brand, Transferpette Integra, Pipetboy 2
Microwave	Siemens
Vortexers	Scientific industries, Vortex genie 2 Roth, Mini Vortex
Shaking Incubator	GFL
Water Bath	GFL
Safety Cabinet	Thermo Scientific, Safe S2020
Gel Electrophoresis	VWR, MINI GEL II
Power Pac 200	BioRad
Electroporation device	MaxCyte, ExPERT GTx

FACS device	BD FACSCalibur™ Flow Cytometer
Microscope	Leica, DMi1
Laboratory scale	Ohaus, E400 D
Gel Analyser	LI-COR, Odyssey Fc
Hemocytometer	La fontaine, Neubauer Improved
Bunsen burner	Carl Friedrich Usbeck
Incubator	Thermo Scientific™, HERA cell
Cell freezing container	Thermo Scientific™, MrFrosty™

2.2.2 Consumables

Table 2 List of consumables

Article	**Manufacturer**
Pipette tips	Biozym, SurPhob Eppendorf, epT.I.P.S. standard, biopur Peqlab, peqGOLD safeguard Starlab, TipOne
Sealing Film	Sigma Aldrich, Parafilm M (P7793-1EA)
Electroporation Cuvettes	Maxcyte, R-50x3 expert
Falcon tubes	Greiner bio-one
Tubes	Eppendorf, Safe-Lock Tubes 0,5ml, 1,5ml, 2ml (normal and Biopur)
Cell culture flasks	Greiner, BioOne Cellstar (250ml , 550ml)
Filter Flasks for Bacterial Preculture	Thermo Scientific™, Sterile Disposable PETG Flask Plain Bottom with Vented Closure
Cell culture plates	Greiner, Cellstar 6 well cell culture plate

2.2.3 Chemicals, reagents and kits

Table 3 List of chemicals, reagents and kits

Article	**Manufacturer**
DNA isolation kit	Macherey-Nagel, NucleoSpin tissue kit
DNA purification kit	Qiagen, QIAquick PCR purification kit
Poly A kit	invitrogen, Poly(A) tailing kit
mRNA production kits	Thermo Fisher Scientific, MEGAscript™ T7 ranscription kit Thermo Fisher Scientific, mMESSAGE mMACHINE™ SP6 transcription kit
Restriction enzyme	BioLabs GmbH, PME I Enzyme
EDTA	Sigma Life Science
Ethanol absolute	PanReac AppliChem ITW Reagents
Nuclease-free water	Ambion, DEPC-Treated Water
Gel electrophoresis buffer	invitrogen, UltraPure™ 10X TAE Buffer
Nucleic acid gel stain	Biotium, GelRed 10000X in water
Agarose	invitrogen, UltraPure™ Agarose - 1000 (for mRNA) Lonza, SeaKem LE Agarose (for DNA)

Gel loading dye	NEB, Gel Loading Dye, Purple (6X)
1 kb DNA ladder	NEB, 1 kb DNA Ladder
100bp DNA ladder	NEB, Quick-Load® 100 bp DNA Ladder
RNA gel ladder	NEB, single stranded RNA (ssRNA) Ladder
PBS (Phosphate buffered saline)	Sigma Life Science, Dulbecco's Phosphate Buffered Saline
Electroporation Buffer	Maxcyte, HyClone™ Electroporation Buffer
RPMI Medium	Sigma Life Science, RPMI-1640 Medium
FBS (fetal bovine serum)	Gibco™, FBS Value 500 ml (A5256701)
L-Glutamine	Sigma Life Science, L-Glutamine solution, 200 mM, solution, sterile-filtered, BioXtra, suitable for cell culture
Penicillin & Streptomycin	Sigma-Aldrich, Penicillin-Streptomycin (P0781-100ml)
Ampicillin	Carl Roth, Ampicillin Natriumsalz 25 g, ≥97%, BioScience Grade
LB Medium	Carl Roth, LB Medium (Lennox) for molecular biology
Plasmid Preparation kit	Qiagen, EndoFree Plasmid Maxi Kit (10)
ARCA (Anti-Reverse Cap Analog)	ThermoFisher Scientific Jena Bioscience
PCR Enzyme	Promega, GoTaq G2 Master Mix

SCF	Miltenyi Biotec, Human SCF, research grade
TPO	Miltenyi Biotec, Human TPO, research grade
Flt3-Ligand	Miltenyi Biotec, Human Flt3-Ligand, research grade
HSC Supplement	Miltenyi Biotec, HSC Brew Medium Supplement
Human Serum Albumin (HSA)	Octapharma, Human Serum Albumine, 25%, Pharmaceutical Grade
HSPC medium for maintenance	Miltenyi Biotec, HSC-Brew GMP Medium
HSPC medium for expansion	Miltenyi Biotec, StemMACS™ HSC Expansion Medium XF, Human
IL-3	Miltenyi Biotec, Human IL-3, research grade
CD34 Antibody	Miltenyi Biotec, CD34 Antibody, anti-human, APC
CD45 Antibody	Miltenyi Biotec, CD45 Antibody, anti-human, FITC, REAfinity™
RNaseZap	Sigma Life Science

2.2.4 Cells

Table 4 List of cells used for transfection

Cell type	**Source**
K562 cells	Sigma-Aldrich

HSPCs	Healthy donors

2.2.5 Software

Table 5 List of used software

Program	**Version**
FlowJo	10.8.0
ApE- A plasmid Editor	v2.0.49.10
Image Studio	Ver 4.0
ICE CRISPR Analysis Tool (Synthego)	-
GraphPad Prism	Version 10.1.1 (323)
Biorender	-
pegFinder (http://pegfinder.sidichenlab.org/)	-

2.2.6 Primer Sequences

Primers were designed with the Primer-Blast tool from www.ncbi.nlm.nih.gov. Specifications for the primers used in the project are listed in **Table 6**.

Table 6 List of primers

Gene	Fwd/Rev	Sequence (5' -> 3')
ARSA	Forward	CCC CGT GAC CCC TGA CT
	Reverse	ATC AGG CCA CAA ACC CCC TC
IL2RG	Forward	AGG CCA CAC AGA TGC TAA AAC T
	Reverse	TGC TAC ATT CAC GTC CCT AGT

2.2.7 Plasmids

Plasmids of **pCMV-PE2 (PE2)** and **pCMV-PE2-P2A-GFP (PE2-GFP)** (Anzalone et al., 2019) were bought from Addgene (pCMV-PE2 #132775; pCMV-PE2-P2A-GFP #132776) (https://www.addgene.org).

pCS2+ DsRed Plasmid was a gift from Prof. Michael Kormann.

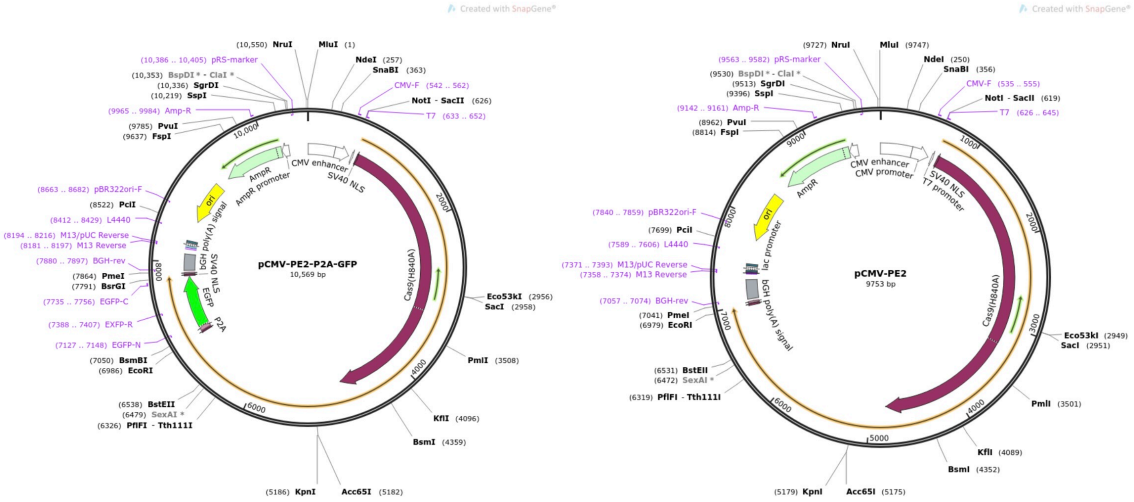

Figure 3 Plasmid map for PE2 & PE2-GFP (created with SnapGene) (Find this picture in large in the section Appendix **A1**)

2.2.8 pegRNAs and sgRNAs

2.1.8.1 *ARSA* P426L

To design the pegRNA and sgRNA for inducing *ARSA* P426L mutation, pegFinder software was used (http://pegfinder.sidichenlab.org/).

With the recommendations from pegFinder we designed the pegRNA as follows:

Table 7 pegRNA specifications

sgRNA	GACAGGTCATAGAGCAGCGG
RT template (13 nucleotides)	TCATGAGCCCCTG
Primer binding site (12 nucleotides)	CTGCTCTATGAC
Sense 3' extension	TCATGAGCCCCTGCTGCTCTATGAC
Full-length pegRNA	GACAGGTCATAGAGCAGCGGGTTTTAGAGCTAGAAATAGCAAGTTAAAATAAGGCTAGTCCGTTATCAACTTGAAAAAGTGGCACCGAGTCGGTGCTCATGAGCCCCTGCTGCTCTATGAC
PE3 nicking sgRNA	TGGTGAGAACTACAACCTGC

PegRNA and sgRNA were then ordered from *Integrated DNA Technologies* in the form of Custom Alt-R gRNA, 2 nmol (pegRNA) and Alt-R CRISPR-Cas9 sgRNA, 2 nmol (PE3 nicking sgRNA).

2.2.8.2 *IL2RG* c.458T>C

pegRNA to induce *IL2RG* c.458T>C was designed by Yujuan Hou from our research group before this project (Hou et al., 2022). Complementary PE3 nicking sgRNA was designed with pegFinder.

PE3 nicking sgRNA: TTCAGGATCCTGACTTGTCT

2.3 Methods

2.3.1 Plasmid Preparation

2.3.1.1 LB Medium

LB (Lysogeny broth) medium was dissolved in millipore water (25 g/L) and then autoclaved. Ampicillin was added so that the concentration of Ampicillin in medium was 1 µl/ml.

2.3.1.2 Preculture

Glycerol stock of the bacteria carrying the PE2 / PE2-GFP plasmid was taken out of -80^{o}C freezer. A clump of bacteria was scraped off the frozen glycerol stock using a 100 µl pipette. The tip together with the bacteria was transferred to a culture flask with filter lid filled with 25 ml medium. The flask was then transferred to the shaking incubator and incubated at 37^{o}C for 6 hours.

2.3.1.3 Overnight Culture

The preculture was transferred to an Erlenmeyer Kolben filled with 200 ml medium, closed loosely to allow air to enter, then transferred to the shaking incubator for overnight incubation.

2.3.1.4 Maxipreparation

QIAGEN Plasmid Maxi Kit was used. Bacterial cells were harvested by centrifugation at 6000g for 15 minutes at 4^{o}C. Bacteria are resuspended in 10 ml Buffer P1. Then 10 ml Buffer P2 was added and mixed thoroughly by vigorously inverting the tube 4-6 times followed by 5 minutes incubation at room temperature. It was important to avoid vortexing (risk of shearing damage to genomic DNA) and not letting the incubation proceed for more than 5 minutes. Resulting mixture should appear homogeneously colored with no cell clumps. Then 10 ml of chilled Buffer P3 was added and the falcon immediately and thoroughly inverted 4-6 times again followed by 20 minutes incubation on ice. The mixture was then filtered using QIAfilter cartridges. In the meantime, a QIAGEN-tip 500 column was equilibrated by applying 10 ml Buffer QBT and allowing the column to empty by gravity flow. The filtered supernatant was then applied to the QIAGEN-tip directly after filtration. Then the QIAGEN-tip was

washed with 2 x 30 ml Buffer QC. DNA in the tip was eluted with 15 ml Buffer QF and the eluate was collected in a 50 ml falcon. DNA was precipitated by adding 10.5 ml room temperature isopropanol to the eluate, followed by centrifugation at ≥15,000 g for 30 minutes at 4°C and removal of the supernatant by everting. Resulting DNA pellet was washed with 5 ml of room-temperature 70% ethanol and centrifuged again at ≥15,000 g for 10 minutes at 4°C. The supernatant was removed by everting and the pellet air-dried for 5-10 minutes. The pellet was then eluted in a suitable amount of Buffer TE. Concentration was measured with nano drop. The plasmid size and integrity was analyzed on gel and the correct sequence confirmed by Sanger sequencing.

2.3.1.5 Creating Glycerol Stock

Glycerol stock was created by taking 500 µl of the bacterial culture after overnight incubation and mixing it with 500 µl of 50% Glycerol inside a cryovial. It was stored at -80°C.

2.3.2 Plasmid Linearization

The following reagents were prepared in a 1.5 ml Eppi (Eppendorf tube) on ice:

Table 8 Plasmid linearization reaction

Component	Amount
Nuclease-free water	40-X µl
Plasmid	X µl (10 µg)
Restriction Enzyme (pMeI / XbaI)	5 µl
rCutSmart buffer	5 µl
Total	**50 µl**

The **pMeI** and **XbaI** restriction enzymes were used for linearization of PE2/PE2-GFP and the DsRed plasmid respectively.

The mixture was incubated at 37°C for 1 hour. The enzyme was then heat-inactivated at 65°C for 20 minutes. Before clean-up, 1 µl of each sample was

isolated for gel electrophoresis on DNA gel next to non-linearized sample to verify success of linearization process.

Clean-up process was as follows: The reaction was terminated by adding 1/20th volume of 0.5 M EDTA, 1/10th volume of 3 M Sodium acetate or 5 M Ammonium acetate, 2 volumes of ethanol. After mixing well with a pipette, the reaction mix was chilled at -20°C for at least 15 minutes. DNA was then pelleted in a microcentrifuge at top speed (20817 g) for 20 minutes at room temperature. Supernatant was carefully removed with a pipette followed by another round of centrifugation for 2 minutes and removal of remaining supernatant.

Resulting linearized plasmid was then resuspended in 10 µl nuclease-free water and concentration was measured with NanoDrop™. Samples were labeled and stored at -20°C.

2.3.3 IVT mRNA Production

Following components were used for IVT (in vitro transcription) mRNA (messenger RNA) production:

- MEGAscript T7 transcription kit (Thermofisher)
- ARCA (Thermofisher / Jena Bioscience)
- Poly-A tailing kit (Thermofisher)
- Linearized plasmid

Before starting, the area and instruments used for production were cleaned thoroughly with 70% Isopropanol and RNaseZap. The reagents were thawed on ice, then vortexed and spun down. The reaction was then prepared in 1.5 ml Eppendorf Biopur tubes as follows:

Table 9 Pipetting scheme for mRNA production

Component	Amount
Nuclease-free water	5-X µl
ATP solution	2 µl
CTP solution	2 µl
UTP solution	2 µl
GTP solution (1:5 stock dilution)	2 µl

ARCA	3 µl
10X Reaction buffer	2 µl
Plasmid DNA (1 µg)	X µl
Enzyme mix	2 µl
Total	**20 µl**

The reagents were then mixed gently by pipetting up and down and spun down with a microfuge. After that, Eppis were sealed with parafilm and placed into a block-heater at 37°C for 2 hours. Next, 1 µl of Turbo DNase was added to each sample and incubated at 37°C for 15 minutes. For Poly-A tailing, the following reagents were added to each sample:

Table 10 Pipetting scheme for Poly-A tailing

Component	Amount
Nuclease-free water	36 µl
5X E-PAP buffer	20 µl
25 mM $MnCl_2$	10 µl
1 mM ATP	10 µl
Total	**96 µl**

The reagents were mixed by gently pipetting up and down. Then, 0.5 µl of each sample was taken to a PCR (polymerase chain reaction) tube and kept at -20°C as non-polyadenylated control for gel electrophoresis. After that, **4 µl of E-PAP enzyme** were added to each sample, then mixed gently. Tubes were again put to the heater at 37°C for 1 hour.

For Clean-up, the reaction was stopped by adding 30 µl LiCl Precipitation Solution and 30 µl Nuclease-free water. The samples were then vortexed thoroughly and transferred to -20°C for at least 30 minutes. After that the mRNA was pelleted with the centrifuge for 25 minutes at maximum speed (20817 g). The pellet was then washed with 1 mL 70% ethanol and re-centrifuged for 5 minutes at maximum speed. The ethanol was then again removed in the same

manner and the mRNA resuspended in Nuclease-free water (20-30 µl). The concentration was determined with NanoDrop, the samples were aliquoted and transferred to -80°C.

To check for size and polyadenylation, adenylated and non-adenylated samples were run on gel as described in section ***2.3.13 Gel Electrophoresis***.

2.3.4 Cell handling

2.3.4.1 K562 cells

Frozen K562 cells were taken from N_2 tank and thawed in the water bath until the ice in the cryovial has almost completely melted. The cells were then transferred into 10 ml of fresh medium for culturing K562 cells, consisting of RPMI1640 medium with 10% FBS, 1% L-glutamine and 1% P/S (Penicillin/ Streptomycin). After centrifugation (5 minutes at 400 g) and removal of supernatant, the cell pellet was dissolved in 10 ml of K562 medium, transferred to a suitable flask and put to the incubator at 37°C with 5% CO_2.

Every second day, cells were counted and split if necessary. If higher cell numbers were needed prior to transfection day, cells were given more media and transferred to a bigger flask.

2.3.4.2 HSPCs

Frozen HSPCs were taken from N_2 tank and thawed in the water bath until the ice in the cryovial has almost completely melted. The cells were then transferred into 10 ml of fresh HSC-Brew GMP medium without any supplements and centrifuged for 15 minutes at 300 g. The cells were then resuspended in 1-2 ml of preheated HSPC maintenance medium (see **Table 11**). After counting, maintenance medium was added to get a cell density of 1 million cells / ml and cells were transferred to 24 or 48 well plates at portions of 2 ml and 1 ml per well respectively. Plates were then transferred to the incubator at 37°C with 5% CO_2.

After electroporation, HSPCs were seeded in a specific HSPC differentiation media (**Table 12**). Stock concentrations for cytokines used in the preparation of media is shown below in **Table 13**.

Table 11 Protocol for HSPC maintenance medium

Component	Amount
HSC-Brew GMP Medium	15 ml
HSC Supplement	150 µl
HSA (Human Serum Albumin)	1.32 ml
Flt3 (Human Flt3 Ligand)	62 µl
SCF	45 µl
TPO	14 µl

Table 12 Protocol for HSPC differentiation medium

Component	Amount
StemMACS™ HSC Expansion Media	10 ml
Penicillin &Streptomycin	100 µl
L-Glutamine	100 µl
SCF	10 µl
IL-3	50 µl
	(Day 0-3)

Table 13 Stock concentrations of cytokines for HSPC medium

Cytokine	Stock
M-CSF	80 ng/µl
GM-CSF	80 ng/µl
SCF	100 ng/µl
IL-3	20 ng/µl
TPO	20 ng/µl
Flt3	100 ng/µl

2.3.4.2.1 HSPC purity measurement by flow cytometry

One day after thawing the HSPCs, purity of the HSPCs was confirmed by Fluorescence activated cell sorting (FACS). 30 µl corresponding to 3 samples (Control + CD34 + CD45) were taken to a 1.5 ml Eppi. 500 ml PBS were added before centrifuging for 15 minutes at 300 g. Supernatant was removed and the cells resuspended in 100 µl phosphate buffered saline (PBS). 100 µl were transferred into each of 3 FACS tubes. 0.5 µl of CD34 or CD45 antibody were added to their respective samples and mixed carefully. The samples were then incubated for 10 minutes in the dark. Then 1 ml PBS was added to each sample before centrifuging again for 15 minutes at 300 g. Supernatant was removed by everting and the remaining samples were filled up with 100 µl PBS each and taken for analysis with FACS.

2.3.5 Transfection by electroporation

To deliver the prime editing components and DsRed mRNA to the cells, MaxCyte ExPERT GTx electroporation system and R-50x3 cuvettes were used. In each cuvette, 3 samples containing up to 2.5 million cells each, could be transfected. Preset EP programs „K562“ and „HSC3“ were used to process the corresponding cell type. For both cell types, 1 million unprocessed cells were seeded at post-EP culture conditions as control samples.

Transfected reagents were the same for K562 cells and HSPCs (**Table 14**)

Table 14 Reaction components for electroporation of K562 and HSPCs

Sample Type	Component	Amount
Ds Red control	DsRed mRNA	5 µg
PE2	pegRNA	150 pmol
	PE2 mRNA	5 µg
PE2-GFP	pegRNA	150 pmol
	PE2-GFP mRNA	5 µg

PE3 / PE3-GFP	pegRNA	150 pmol
	PE2 / PE2-GFP mRNA	5 µg
	sgRNA	150 pmol

2.3.5.1 K562 cells

On transfection day, cells were counted for number and adequate viability (> 90%). Electroporation device was turned on, program „K562 cells“ was selected and device was charged once with an empty cuvette to prevent long charging with the actual samples. Then the needed 6-well plates were put to the incubator to preheat. 7.5 million K562 cells were centrifuged in a 50 ml falcon tube for 5 minutes at 400 g. Supernatant was then removed. Cells were washed twice with 2 ml of EP buffer, each washing step was followed by a 5 minute centrifugation step at 400 g and removing of supernatant. After removing the supernatant for the last time, the cells were resuspended in a final volume of 150 µl (number of EP chambers x 50 µl). During the last centrifugation step, pegRNA, mRNA and sgRNA (in case of PE3) were taken from -80°C and put on ice. After resuspension of the cell pellet in the final amount of EP buffer, reaction components for each sample were mixed according to **Table 14** within a 0.5 µl Eppi each. Shortly after, 50 µl were taken from the cell suspension, transferred to the corresponding Eppi containing pegRNA, mRNA and sgRNA. Mixing was done by pipetting 2-3 times up and down inside the Eppi before transferring the mixture to its corresponding chamber inside the EP cuvette. When all chambers were filled, the cuvette was processed with the EP device.

Samples were transferred to their respective wells in the prepared 6-well plates. EP chambers were washed once with 50 µl EP buffer, which was also transferred to the wells. It was very important that the sample together with the EP buffer formed a stable drop in the middle of the well to prevent drying out during the following recovery phase of 30 minutes at 37°C with 5% CO_2.

After that, 2.5 ml of K562 medium without P/S (to prevent antibiotics to enter the cells while their pores are still open) was added carefully to each plate before transferring the samples back to the incubator.

Four hours later, another 2.5 ml of medium and 50 µl of P/S were added to each well, leading to a final seeding concentration of 1 million cells / ml.
Samples were cultured at 37°C with 5% CO_2 until DNA isolation. Density of the culture and color of the pH-indicating medium was checked after two days to see if the cells needed more medium.

2.3.5.2 HSPCs

Two days after thawing, HSPCs were counted for number and viability. The number of cells used per sample varied between 2 and 2.5 million cells, depending on the output of the thawed vials. Viability had to be ≥90% to proceed with transfection. 6-well plates were filled with HSPC expansion medium so that the seeding concentration after transfection would be 0.5 million cells / ml and subsequently put in the incubator at 37°C with 5% CO_2 to preheat. Electroporation device was charged once with an old cuvette to avoid long charging time for the cuvettes containing the samples. Only one cuvette was processed at a time to avoid reagents being at room temperature for a long time or the cells being out of the incubator for too long.
The cells needed for one cuvette were isolated from the maintenance culture and transferred to a 50 ml falcon. Then they were centrifuged for 10 minutes at 300g with break setting at 6 (same settings for all centrifugation steps). Supernatant was removed by everting and the cells were washed with 2 ml of PBS. After that followed another centrifugation, removing supernatant, washing with 2 ml of EP buffer and again centrifugation. At last, supernatant was removed and the cells were resuspended with 150 µl (3 samples x 50 µl) of EP buffer.
Reagents for transfection were taken from -80°C and put on ice during the last step of centrifugation. After resuspending the cells in final amount of EP buffer, reagents were centrifuged and the reaction components were set up according to **Table 14** in 0.5 ml Eppis. After that, 50 µl of cell suspension were transferred to the first reagent Eppi, mixed by carefully pipetting up and down before getting transferred to the first EP chamber of the cuvette. This was repeated for the other 2 wells and the cuvette was transferred to the EP device. After EP, the cuvette was transferred to the incubator for 15 minutes at 37°C with 5% CO_2 to

recover. After that, the samples were transferred to their respective wells of the 6-well plate containing preheated expansion medium by first transferring the content of a cuvette chamber, then washing the chamber with 50 µl of electroporation buffer and likewise transferring that to the 6-well plate before putting the plates back to the incubator. Four hours after seeding the cells, antibiotics were added to the culture as stated in the recipe for HSPC differentiation medium (**Table 12**). This was done to avoid the antibiotics to enter the cells through open pores after EP. The plates were cultured at 37°C with 5% CO_2 until DNA isolation. No more medium was added.

2.3.6 Determining transfection efficiency

One day after electroporation, transfection efficiency was determined by measuring expression of DsRed and GFP with FACS. 200 µl of each sample (Control, DsRed, GFP) were transferred to separate FACS tubes and centrifuged to 10 minutes at 300 g. Supernatant was removed, cells were washed with 1 ml of PBS and the tubes were centrifuged again at the same conditions. After removing supernatant for the last time, 100 µl of PBS were added to each sample. Measurements were performed using BD FACSCalibur™ Flow Cytometer. Results were analyzed with FlowJo to quantify DsRed and GFP expression.

2.3.7 DNA Isolation

DNA isolation of transfected cells was carried out on day 3 post EP with the day of EP being day 0. For DNA isolation, 1.25 ml of each sample were used.

DNA isolation was performed using the NucleoSpin Tissue kit.

The cells were transferred to a 1.5 ml tube and centrifuged for 5 minutes at 500 g (10 minutes at 300 g for HSPCs). All following centrifugation steps were carried out for 5 minutes at 11 000 g.

After removing the medium, cells were resuspended in 200 µl of buffer T1, 20 µl Proteinase K and 200 µl Buffer B3. After vortexing, the sample was incubated at 70°C for 13 minutes. After incubation, 210 µl of ethanol (96-100%) were added and mixed vigorously by vortexing. The mixture was then applied to a NucleoSpin Tissue column which was placed in a collection tube. Then the

sample was centrifuged. The collection tube was discarded with the flow-through and the column placed in a new collection tube. Then for the first washing step, 500 µl of Buffer BW was added and the sample was centrifuged again. Flow-through was discarded and the column placed back into the same collection tube. For the second washing step, 600 µl of Buffer B5 were added, then again centrifuged and the flow-through discarded. For drying the silica membrane, another centrifugation step was carried out without any addition. At last, the column was placed into a 1.5 ml tube and 30 µl of nuclease-free water were applied to the membrane of the column. Then the sample was again centrifuged to obtain the dissolved DNA.

DNA concentration was measured with Nanodrop and the samples were labeled and stored at -20°C.

2.3.8 PCR

PCR was used to amplify the desired sequences of *ARSA* and *IL2RG* genes. First, a gradient PCR was performed to determine the correct temperature for the primers. A gradient program was used to enable simultaneous processing of *ARSA* and *IL2RG* samples in different rows of the thermocycler. The pipetting scheme and program for normal PCR and gradient PCR was as follows:

Table 15 Reaction mixture for PCR

Component	Amount
Genomic DNA (100 ng)	X
Forward Primer (5 µMol)	1 µl
Reverse Primer (5 µMol)	1 µl
GoTaqGreen Master Mix	10 µl
Nuclease-free water	8-X µl
Total	20 µl

1. Initial denaturation phase of 2:00 minutes at 95°C
2. 40x repetitions of the following 3 phases:
    - 0:40 minute denaturation at 95°C

- 0:30 minute annealing at temperatures reaching from 53,5°C to 63,9°C
- 1:00 minute elongation at 68°C

3. Infinite Hold at 4°C

For gradient PCR, 8 samples were prepared according to **Table 15** and then placed into the different rows of the Thermocycler, referring to different temperatures. After PCR, samples were run on gel next to a 100 bp (base pair) ladder (**Figure 5**) and the sample with the thickest amplification band was chosen to determine the best temperature for the primers (**Figure 4**).

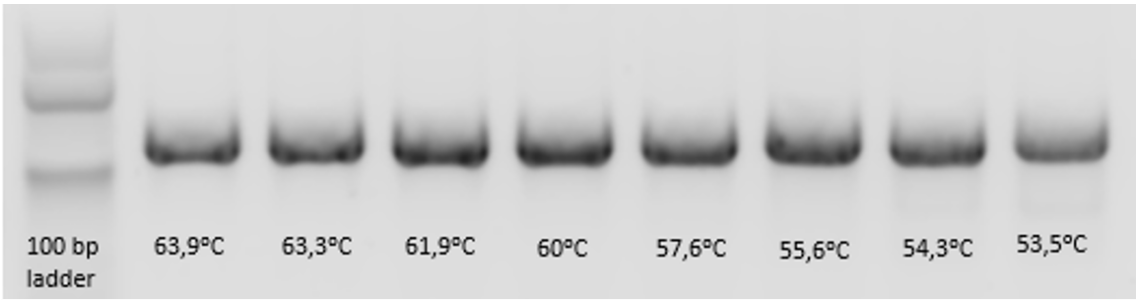

Figure 4 Gel picture of gradient PCR for *ARSA* primers

With 60°C being the thickest band on the gel (**Figure 4**), 60°C was chosen to be the best temperature for our *ARSA* primers.

To amplify the desired region for further processing, *ARSA* samples were placed in the 60°C row, *IL2RG* samples in the 62°C row (Hou et al., 2022) at optimal temperature for their respective primers. Gel electrophoresis was used to confirm successful amplification of DNA by running 3µl of each sample (PCR enzyme mix had dye already included) next to a 100 bp ladder for 30 minutes on DNA gel.

2.3.9 DNA Purification

After PCR, DNA purification was used to clean the samples from reagents to obtain pure DNA. QIAquick PCR purification kit was used according to the included standard protocol.

All centrifugation steps were carried out at 17 900 x g at room temperature.

5 volumes of PB Buffer were added to 1 volume of remaining PCR reaction, then mixed by pipetting. The mixture was transferred to a QIAquick column which was placed in a provided 2 ml collection tube. Then followed the first centrifugation step for 1 minute. The flow-through was discarded and the column placed back into the same collection tube. For washing, 750 µl Buffer PE were added to the column followed by another 1 minute centrifugation. The flow-through was discarded and the column again placed in the same collection tube. To remove residual wash buffer, the column was centrifuged for 1 minute without the addition of any buffer. Afterwards the column was placed into a 1.5 ml Eppi. 30 µl of nuclease-free water was applied to the center of the membrane of the column and centrifuged for 1 minute to elute the DNA.
DNA concentration was measured with Nanodrop and the samples were labeled and stored at -20°C.

2.3.10 Sanger Sequencing

Purified PCR product was prepared as shown in **Table 16** and then sent to Eurofins Genomics for Sanger sequencing.

Table 16 Pipetting scheme for Sanger sequencing

Component	Amount
Genomic DNA (75 ng)	X
Forward Primer (5 µMol)	4 µl
Nuclease-free water	13-X µl
Total	17 µl

2.3.11 Analysis of Editing Efficiency

Results obtained from Sanger sequencing were analyzed using the ICE Analysis tool from Synthego to determine editing efficiency.

2.3.12 Gel Electrophoresis

Gel electrophoresis results were visualized using the *LI-COR Odyssey Fc* and the *Image Studio* software.

2.3.12.3 Different ladders used in the project

Different types of ladders where used to visualize results of different experiments (**Figure 5**):

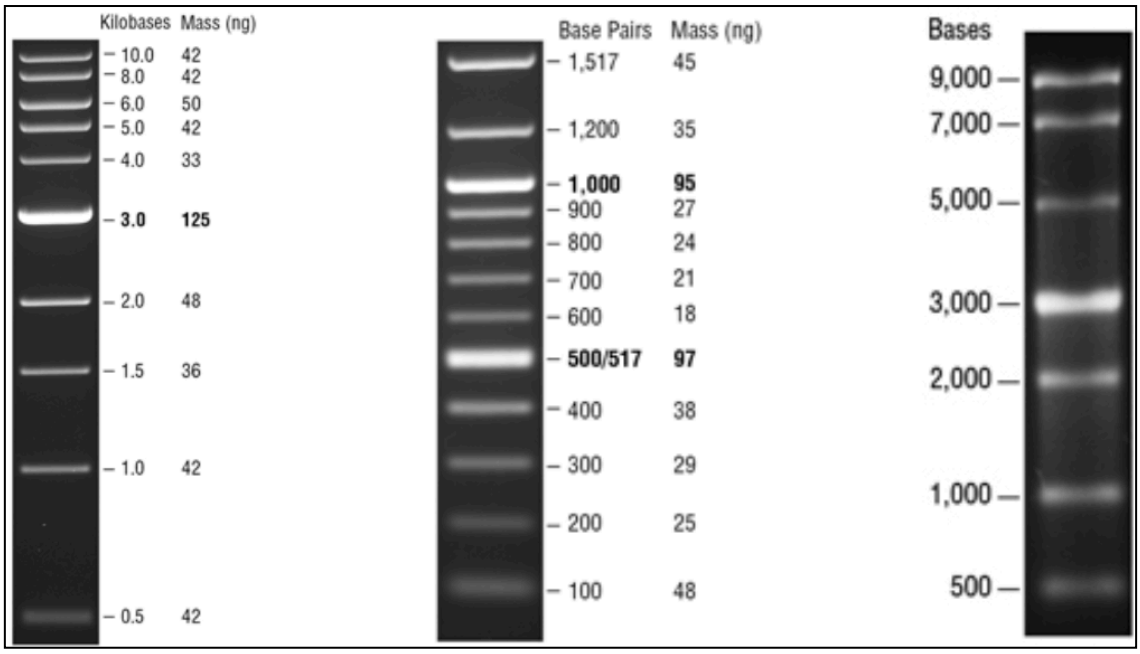

Figure 5 Gel ladders used in the project. From left to right: 1kb DNA Ladder, 100bp DNA Ladder, ssRNA Ladder. (Pictures supplied by New England Biolabs)

3. Results

3.1 Plasmid preparation

3.1.1 PE2 & PE2-GFP

After plasmid preparation, concentrations of circular PE2 and PE2-GFP plasmids were measured with Nanodrop (**Table 16**). Afterwards, plasmids were sent for Sanger sequencing and obtained sequences were matched to the desired sequences in Ape- A plasmid editor. Correct length of the plasmids was also verified via gel electrophoresis (**Figure 6**).

Table 17 Concentrations of circular PE2 & PE2-GFP plasmids

Name	Concentration
PE2 plasmid circular	2758.5 ng/µl
PE2GFP plasmid circular	1807.6 ng/µl

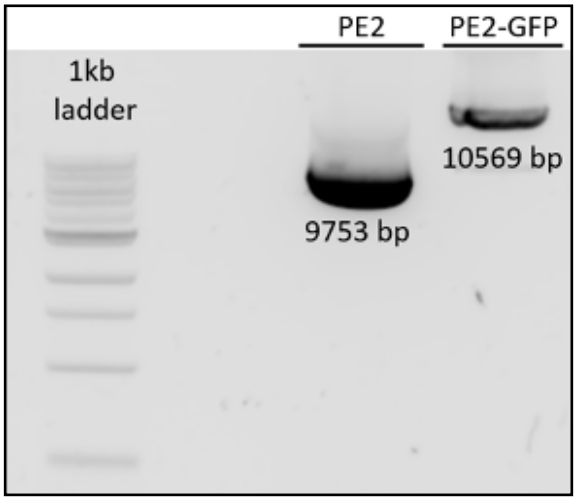

Figure 6 Gel visualization of circular PE2 & PE2-GFP plasmids

3.1.2 DsRed

Circular DsRed plasmid was produced in our research group before this project with a concentration of **1420 ng/µl**.

3.2 Plasmid Linearization

Circular PE2 & PE2-GFP plasmids were linearized using pMeI restriction enzyme. DsRed was linearized using XbaI restriction enzyme. Mean concentrations for all linearized samples that were used for mRNA production are listed in **Table 18.** Success of linearization process was verified using gel electrophoresis (**Figure 7**).

Table 18 Mean concentration of linearized plasmids

Name	Mean Concentration
PE2 plasmid lin.	301.2 ng/µl (n=9)
PE2GFP plasmid lin.	406.7 ng/µl (n=11)
DsRed	373.5 ng/µl (n=4)

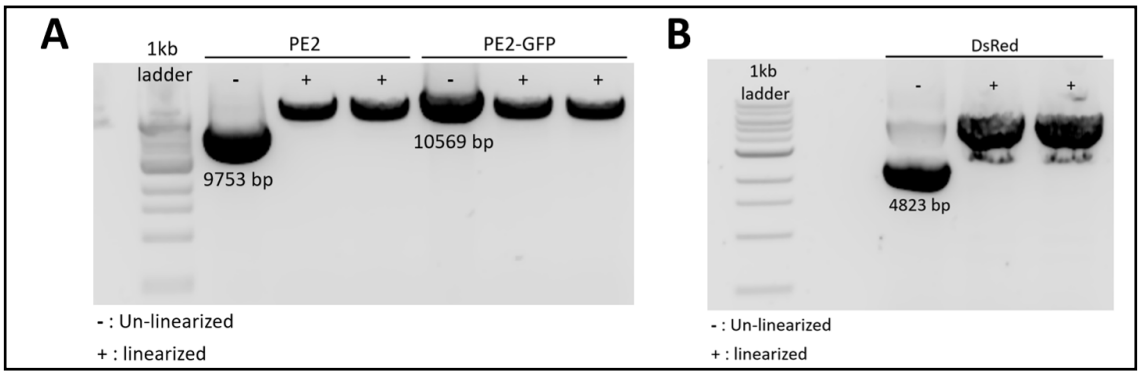

Figure 7 Gel visualization of linearized plasmids. (A) PE2 & PE2-GFP and (B) DsRed plasmid

3.3 mRNA production

For mRNA production of DsRed and PE2 & PE2GFP, different kits were used. DsRed mRNA was produced with mMESSAGE mMACHINE™ SP6 transcription kit, while PE2 & PE2GFP mRNA was produced with MEGAscript™ T7 transcription kit (both manufactured by*ThermoFisher Scientific*). Success of the production and polyadenylation was visualized via gel electrophoresis on

RNA gel (**Figure 8**). Samples with insufficient concentration were discarded. Mean concentrations of mRNA used to transfect cells are listed in **Table 19**.

Table 19 Mean concentration of mRNA used in the project

Name	Mean Concentration
PE2 mRNA	1915.4 ng/µl (n=7)
PE2GFP mRNA	1563.9 ng/µl (n=9)
DsRed mRNA	1519.5 ng/µl (n=4)

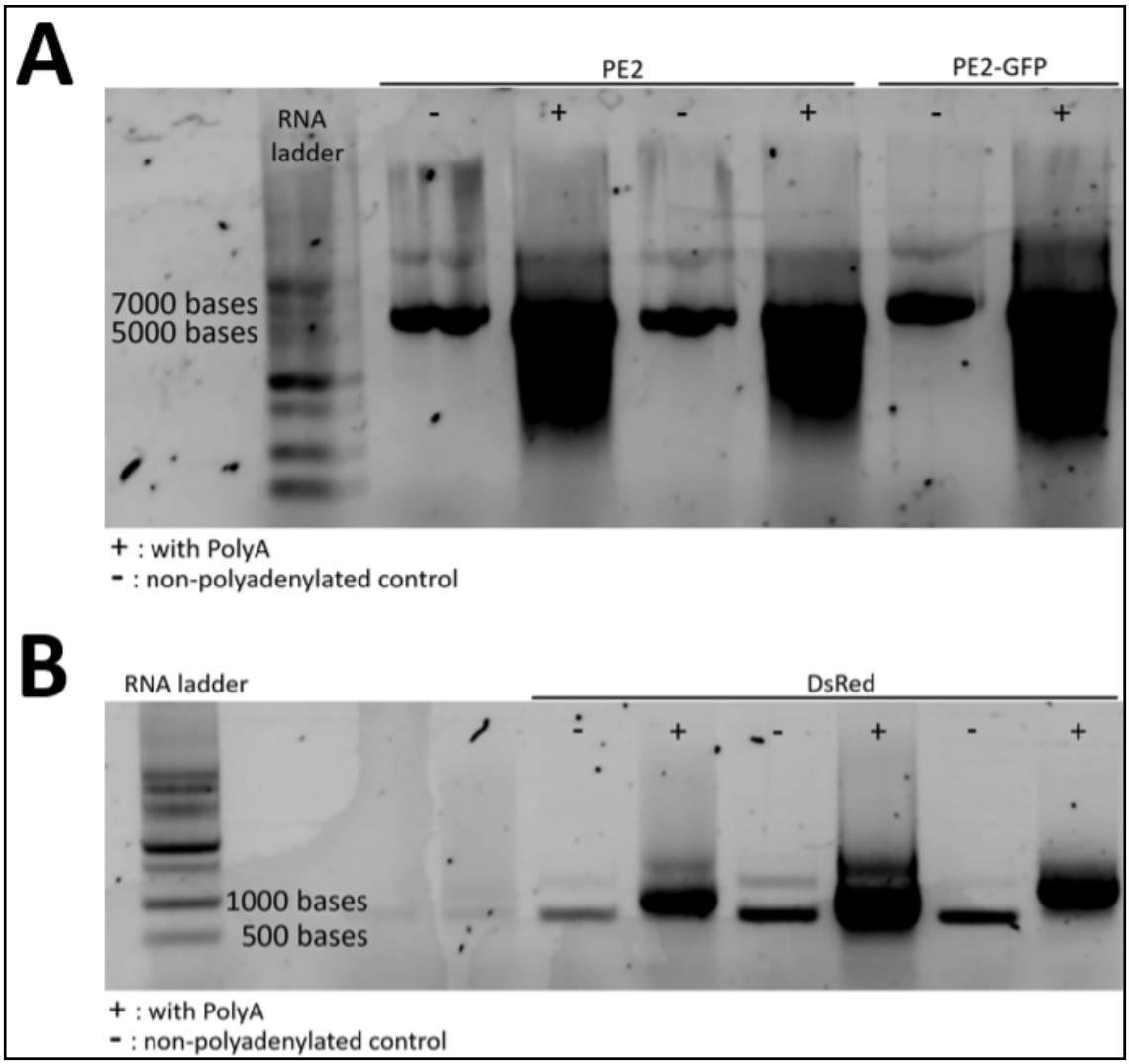

Figure 8 Gel visualization of produced mRNA. (A) PE2 & PE2-GFP and (B) DsRed mRNA next to non-polyadenylated control samples.

3.4 Determining purity of HSPCs

Purity of HSPCs was determined with FACS one day after thawing. CD34 and CD45 antibodies were used to detect the HSPC specific antigens. Results were analyzed with FlowJo (**Figure 9**). Flow cytometry results showed over 99% purity for HSPCs.

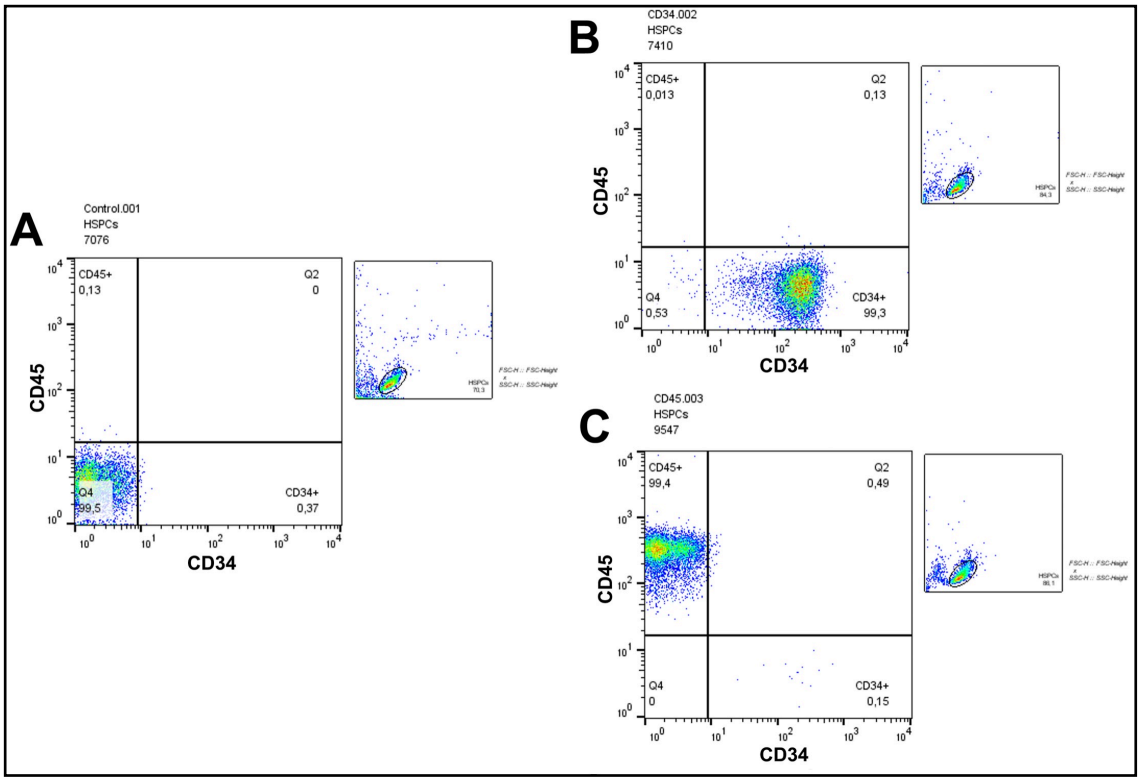

Figure 9 HSPCs purity measured with FACS.

X-axis: CD34 / **Y-axis**: CD45. (A): Unstained control, (B): CD34 stained sample, (C): CD45 stained sample.

3.5 Transfection Efficiency

One day after transfection via electroporation, transfection efficiency was measured using FACS. DsRed mRNA, expressing a red fluorescent protein, was used as electroporation control. Expression of GFP, which was transcribed from PE2-GFP mRNA, was used as a measure of successful transfection and expression of PE2-mRNA. FlowJo visualization of transfection efficiency for

K562 cells and HSPCs is shown in **Figure 10** and **Figure 11**. Graphic presentation of pooled DsRed & GFP expression is shown in **Figure 12**.

The results showed up to **96.3%** GFP expression in K562 cells and up to **54.4%** GFP expression in HSPCs.

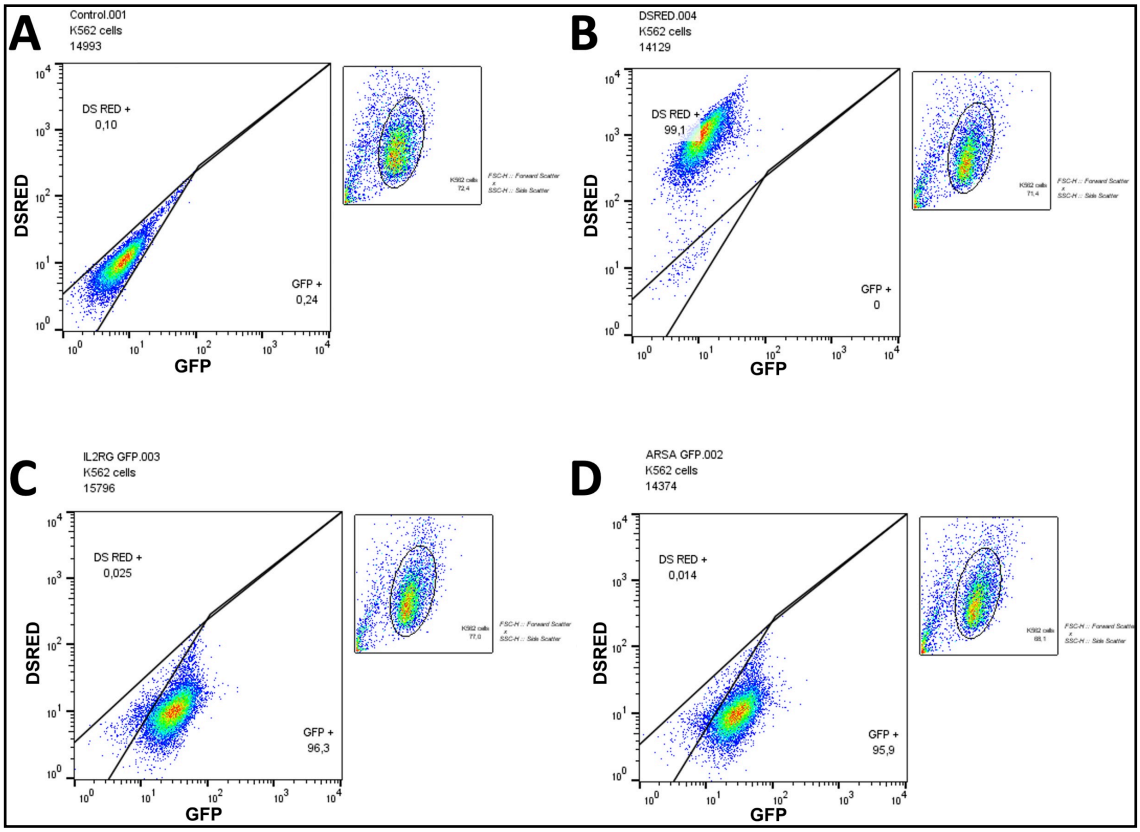

Figure 10 Transfection Efficiency in K562 cells.

X-axis: GFP / **Y-axis**: DsRed. (A) untransfected control, (B) DsRed, (C) PE3GFP + *IL2RG* pegRNA, (D) PE3GFP + *ARSA* pegRNA

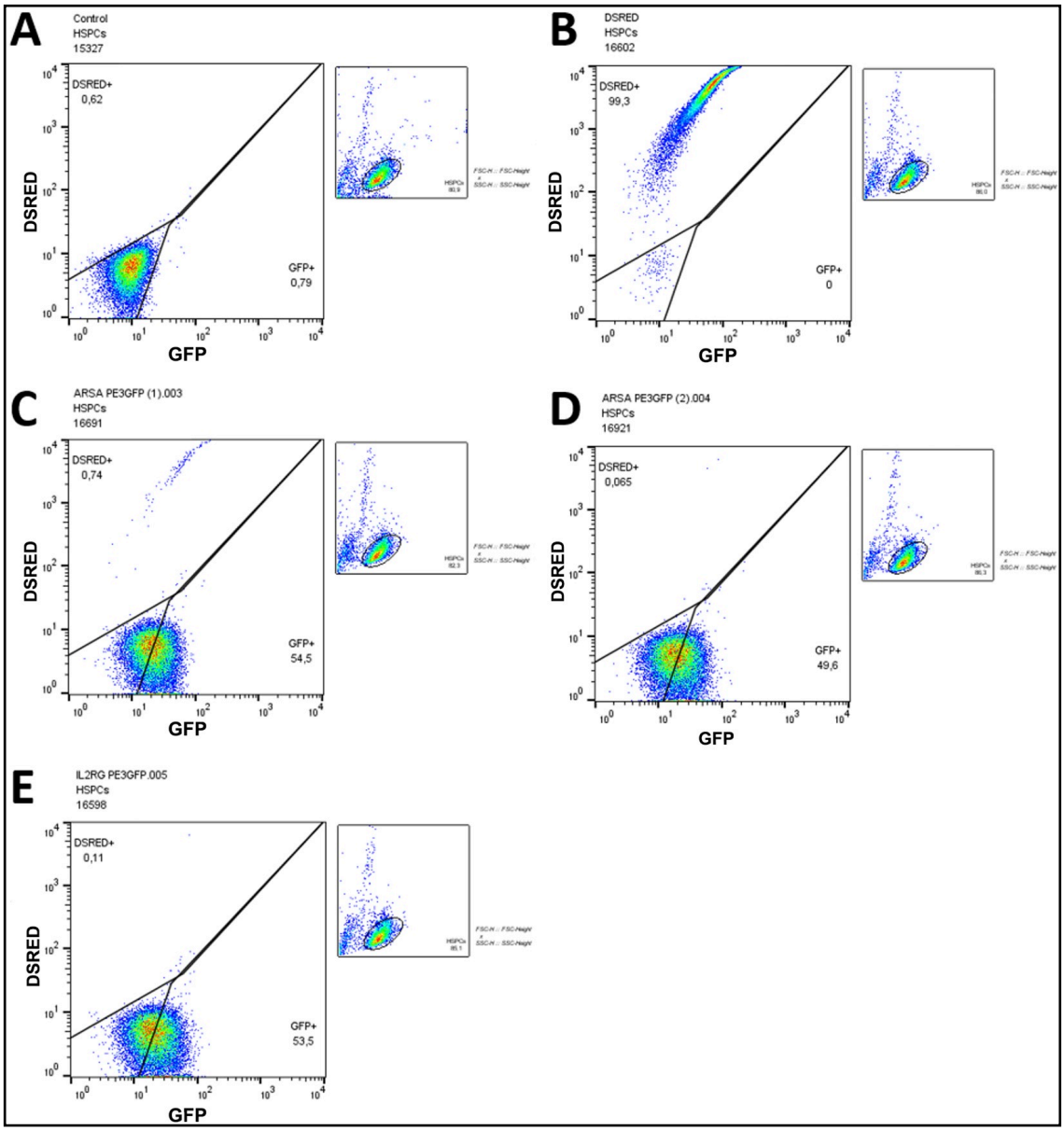

Figure 11 Transfection Efficiency in HSPCs.

X-axis: GFP / **Y-axis**: DSRED (A) untransfected control, (B) DsRed, (C+D) PE3GFP + *ARSA* pegRNA, (E) PE3GFP + *IL2RG* pegRNA

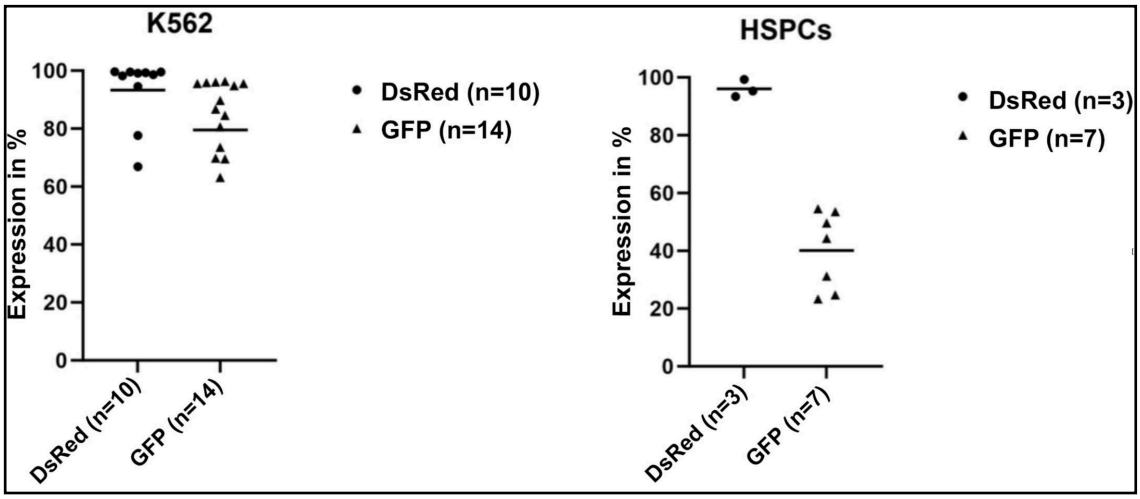

Figure 12 Pooled Transfection Efficiency in K562 cells and HSPCs.

3.6 Processing of DNA

3.6.1 DNA isolation

DNA of transfected and control cells was isolated 3 days after electroporation using Nucleospin Tissue kit. DNA concentration was measured using Nanodrop and wavelength absorbance ratio 260/280 was checked to be in the specific range for DNA samples (Wilfinger et al., 1997) (**Figure 13**).

Sample ID	Date and Time	Nucleic Acid	Unit	A260 (Abs)	A280 (Abs)	260/280	260/230	Sample Type	Factor
IL2RG PE3GFP	28.10.2023 15:43:04	83,2	ng/µl	1,664	0,859	1,94	2,50	DNA	50,00
Control	28.10.2023 15:41:10	281,1	ng/µl	5,621	2,858	1,97	2,36	DNA	50,00
DSRED	28.10.2023 15:42:07	95,7	ng/µl	1,915	0,976	1,96	2,43	DNA	50,00
ARSA PE3GFP	28.10.2023 15:43:58	60,3	ng/µl	1,205	0,611	1,97	2,59	DNA	50,00

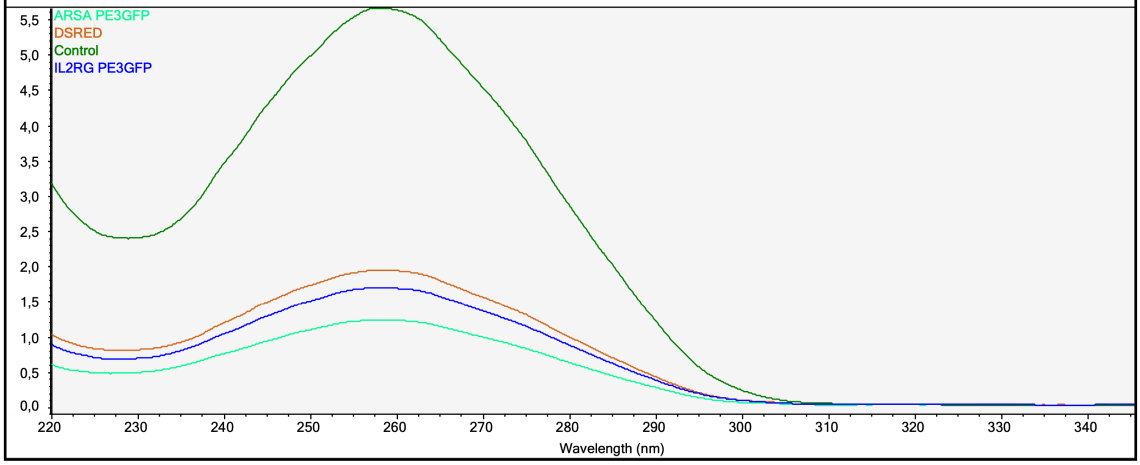

Figure 13 Nanodrop results for DNA isolation of transfected HSPCs

3.6.2 PCR

PCR was performed to amplify desired *ARSA* / *IL2RG* regions. Success of replication was visualized using gel electrophoresis with a 100 bp ladder to check for a band in the correct size of the amplicon (**Figure 14**).

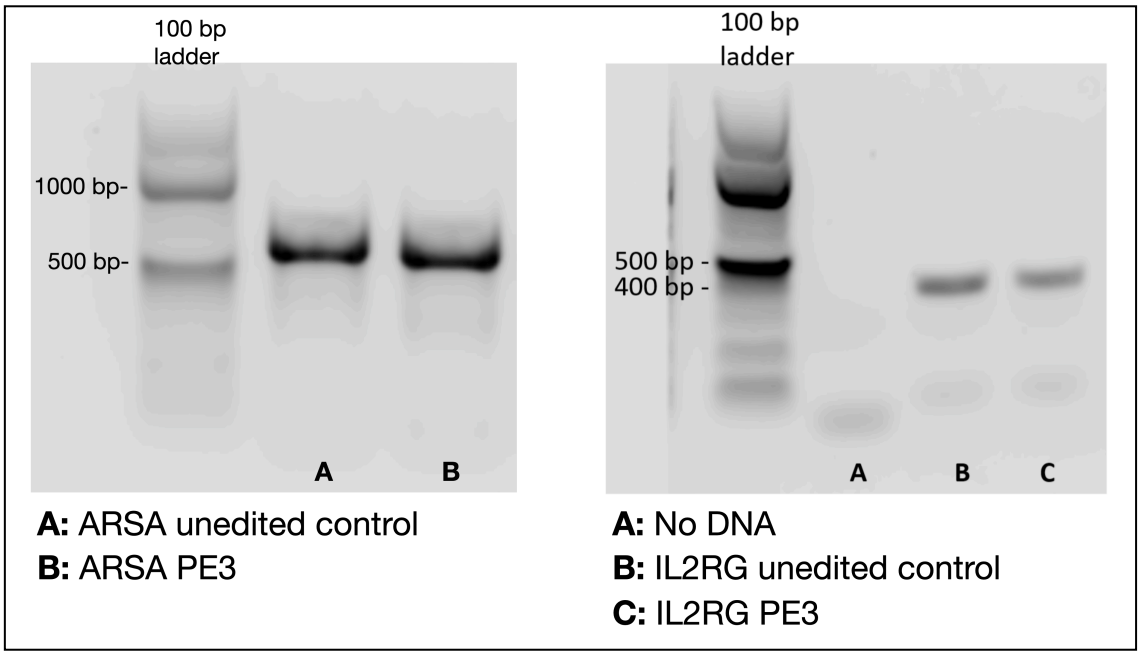

Figure 14 Visualization of PCR results for *ARSA and IL2RG* region

3.6.3 DNA purification

After purification, the concentration of the DNA was again measured using Nanodrop and checked for correct DNA-specific wavelength absorbance ratio 260/280.

3.7 Editing Efficiency

After isolating DNA of the transfected cells and amplifying the desired target regions, samples were sent for Sanger sequencing and the editing efficiency was analyzed by ICE Analysis.

3.7.1 Prime editing for inducing IL2RG c.458T>C mutation

To confirm the effectiveness of the prime editing mechanism utilized in this project, it was first used to induce the *IL2RG* c.458T>C mutation in K562 cells

and HSPCs. This served as a proof of concept, as this locus has been edited successfully already in K562 cells using prime editing (Hou et al., 2022).

Data obtained by Sanger sequencing showed successful induction of the *IL2RG* c.458T>C mutation in both cell types (**Figure 15**). The editing efficiency was then quantified using ICE analysis. Achieved efficiency to induce *IL2RG* c.458T>C mutation was up to **7 %** (PE2) and **30 %** (PE3) in K562 cells and **41 %** (PE3) in HSPCs respectively (**Figure 15**).

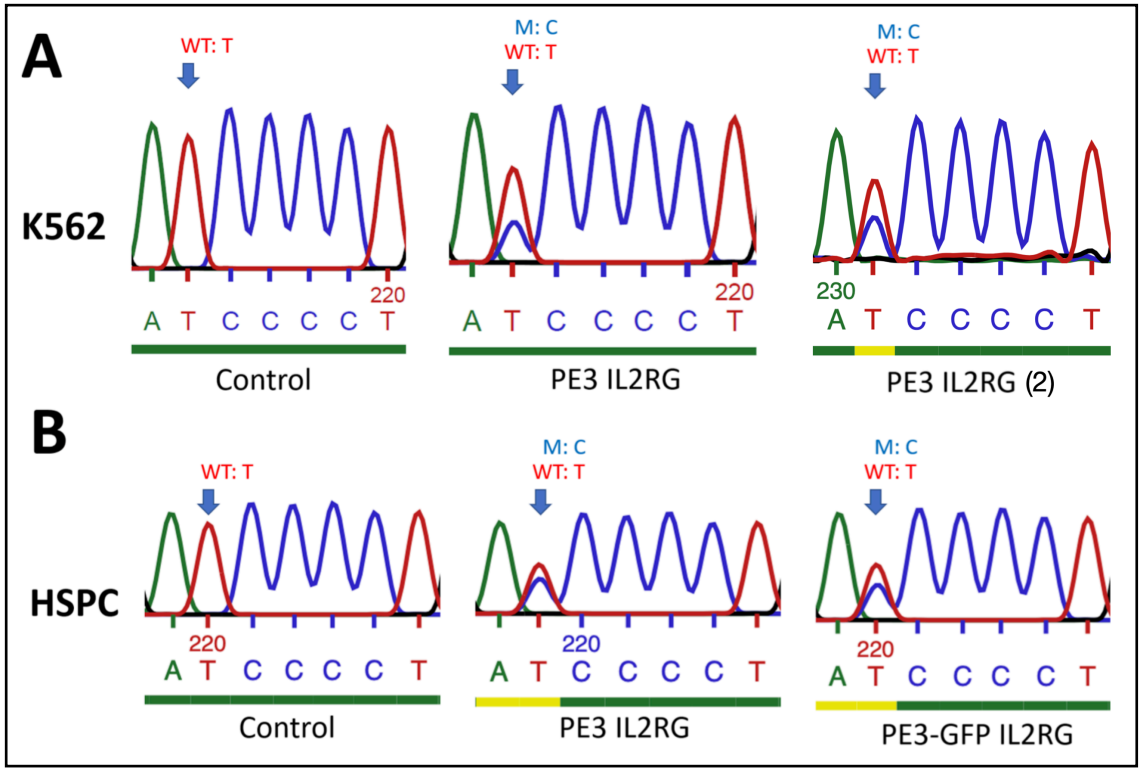

Figure 15 Sequencing data for *IL2RG* transfected samples.

Induction of *IL2RG* c.458T>C mutation was evident in sequencing Data for **(A)** K562 cells and **(B)** HSPCs

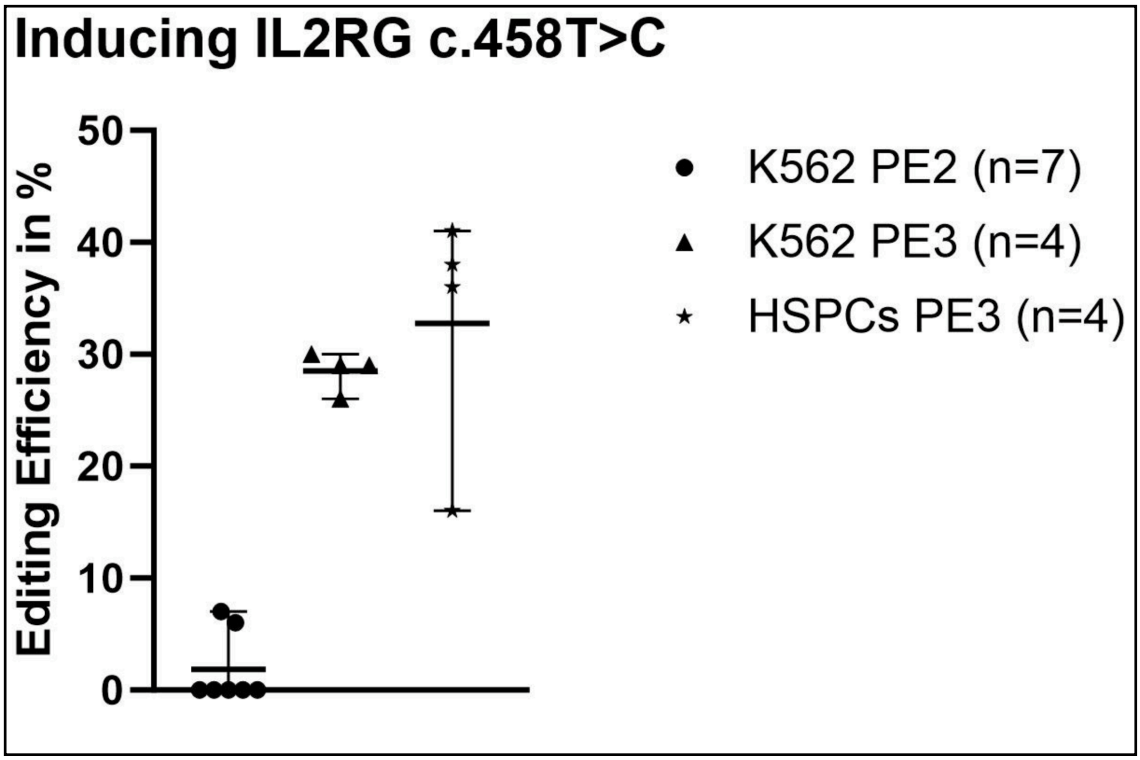

Figure 16 Pooled editing efficiency for *IL2RG* c.458T>C mutation in K562 cells and HSPCs

3.7.2 Prime editing for inducing ARSA P426L mutation

After successfully inducing *IL2RG* c.458T>C mutation in K562 cells and HSPCs, the same prime editors and protocols were used to induce *ARSA* P426L mutation. In the data obtained by Sanger sequencing, editing was visible for K562 cells as seen in **Figure 17**. Further quantification with ICE Analysis showed editing up to **15%** (PE2) and **18%** in K562 cells. In HSPCs however, results showed that no editing has taken place (**Figure 18**).

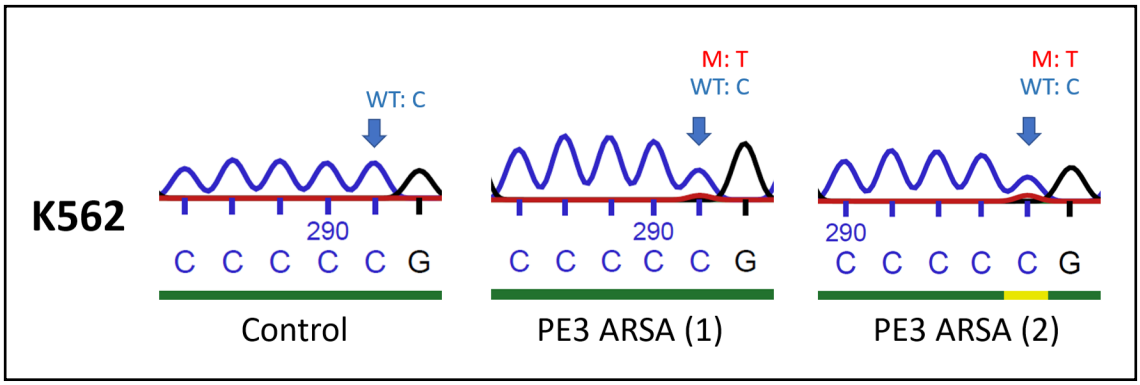

Figure 17 Sequencing data for *ARSA* transfected samples.
Induction of *ARSA* P426L mutation evident in K562 cells.

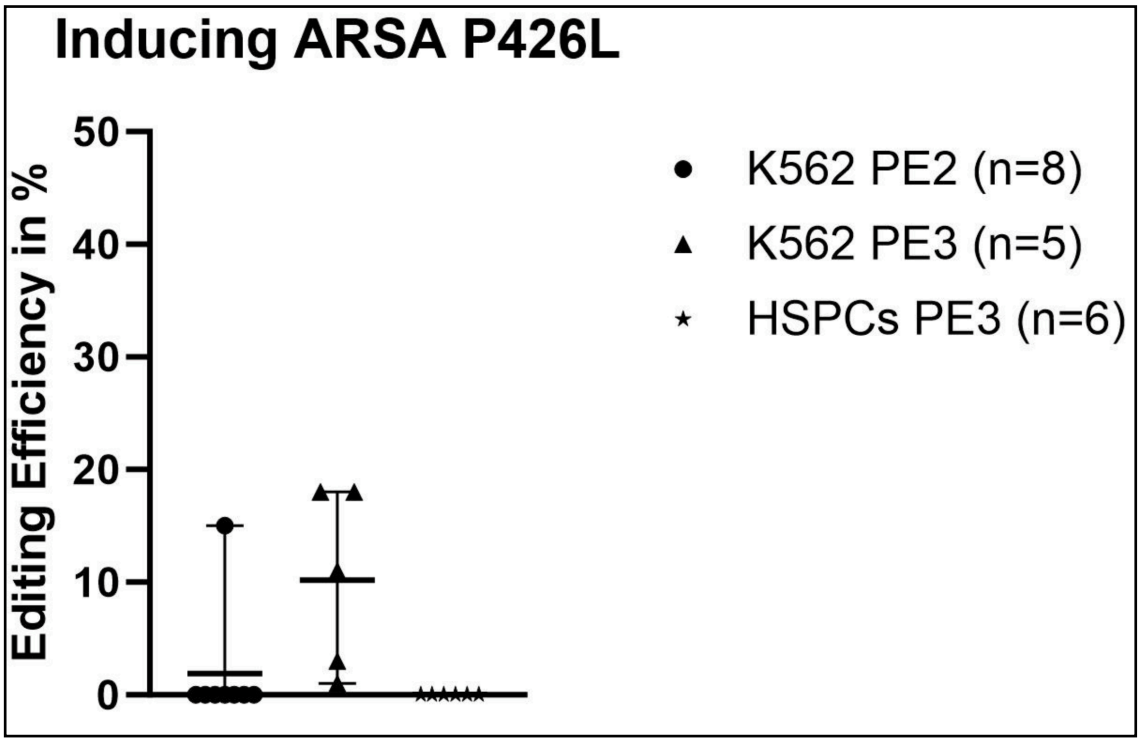

Figure 18 Pooled editing efficiency for ARSA P426L mutation in K562 cells and HSPCs.

3.7.3 Correcting ARSA P426L mutation in patient cells

Since inducing *ARSA* P426L mutation in healthy HSPCs was not successful, we did not proceed to this next step in the project.

4. Discussion

This section addresses the importance and relevance of developing novel therapeutic strategies for MLD, with a particular focus on gene therapy approaches. Further emphasis is placed on the therapeutic potential and technical aspects of gene editing tools, specifically prime editing, to correct *ARSA* P426L point mutation.

4.1 Gene therapy for MLD

Although MLD is a rare disease, its severity and the lack of effective therapy options highlight the need to develop a curative treatment (van Rappard et al., 2015). Therapeutic approaches such as allo-HSCT and ERT have been investigated in the last decade but have shown limited efficacy in slowing, halting, or reversing disease progression reliably (Jonckheere et al., 2023). Currently, the greatest promise lies in the development of gene therapies. One example is Libmeldy, a lentiviral vector (LV)-based gene therapy that introduces *ARSA* with supra-physiological expression into the genome of HSPCs, which are then transplanted back into the patient. This therapy has shown highly encouraging clinical outcomes (Messina & Gissen, 2023). Even though concerns about the risk for insertional mutagenesis have not been confirmed so far (Messina & Gissen, 2023), the long-term safety of this approach remains uncertain as carcinogenesis is a multistep process and potential disruptions to tumor suppressor genes or proto-oncogenes may remain silent for years before additional mutations could potentially lead to the formation of cancer (Kontomanolis et al., 2020). This underlines the need for continued research to develop more precise gene therapeutic methods minimizing long-term risks.

4.1.2 ARSA P426L mutation

The *ARSA* P426L mutation is one of the most common mutations causing MLD. It is mostly associated with the juvenile and adult forms (Lugowska et al., 2005; Rauschka et al., 2006). Due to the slower progression of these forms, there is a larger timeframe before the onset of symptoms to establish host engraftment and restitution of enzyme levels. If newborn screening for MLD would be implemented in the future, as suggested by several authors (Jonckheere et al.,

2023), diagnosis could occur long before symptom onset. For the late onset forms this would mean that there would be years to establish a therapy in a pre-symptomatic stage. One of the main advantages of Libmeldy is the short latency from transplantation to therapeutic effect (Messina & Gissen, 2023), which would not be necessary in that case. While these patients would also be suitable candidates for allo-HSCT, a gene therapeutic intervention which restitutes physiological ARSA activity in patients' HSPCs by correcting the mutation in situ, could be the optimal therapy. A therapy based on precision gene editing would have the advantage that there would be minimized risk of insertional mutagenesis compared to Libmeldy. It would also avoid the risk of developing a Graft-versus-Host-Disease (GvHD), which is a frequent and severe side effect of allo-HSZT.

This makes patients carrying the *ARSA* P426L mutation particularly suitable candidates for therapy approaches based on prime editing and base editing.

4.2 Advantages and limitations of Prime Editing

Prime editing presents a precise tool for editing small nucleotide sequences within the genome (Anzalone et al., 2019). Different publications have described high editing efficiencies when using prime editing approaches to induce a variety of edits in different cell types, including HSPCs (Anzalone et al., 2022; Chen et al., 2021; Kantor et al., 2020; Levesque, 2023; Nelson et al., 2022). For genetic knock-in approaches, prime editing possesses several advantages over CRISPR-Cas9. CRISPR-Cas9 is depending on the cells innate repair mechanisms NHEJ and HDR and induces DSBs that lead to reduced cell viability (Anzalone et al., 2019; Ihry et al., 2018). Compared to base editing, prime editing efficiency is slightly lower but it offers a significantly broader spectrum of editing possibilities and avoids the issue of bystander mutations. Thereby prime editing presents as a more precise and versatile tool for genome editing (Kantor et al., 2020).

Although prime editing has been reported to cause minimal off-target effects (Kantor et al., 2020), recent studies have shown that genotoxic effects can still occur, particularly with PE3 systems. These include off-target edits, larger deletions, and DSBs that may trigger apoptosis. However, such effects appear

to occur less frequently compared to base editing and CRISPR-Cas9 (Fiumara et al., 2023). Research on this topic should be closely monitored in the future to evaluate the effects on a possible application in gene therapy.

4.3 Prime Editing to target *ARSA* P426L mutation in K562 cells and HSPCs

In this study, we employed PE2 and PE3 prime editing systems to target the *ARSA* P426L mutation. As a proof of concept, we also targeted the *IL2RG* c.458T>C site, a locus previously shown to be editable in various cell types (Hou et al., 2022). Electroporation was used as the transfection method, demonstrating high efficiency across all tested cell types, with good post-transfection viability. In K562 cells, the *IL2RG* c.458T>C mutation was successfully introduced with a mean efficiency of 1.86% using PE2 and 28.5% using PE3. In HSPCs, the mean editing efficiency for *IL2RG* c.458T>C using PE3 was 32.75%. In contrast, the *ARSA* P426L mutation was introduced with a mean efficiency of 1.88% (PE2) and 10.20% (PE3) in K562 cells, but editing was not successful in HSPCs.

Reported editing efficiencies in the literature also show considerable variability depending on the target locus and cell type (Anzalone et al., 2022; Chen et al., 2021; Happi Mbakam et al., 2022; Li et al., 2023).

The experiments targeting the *ARSA* and *IL2RG* loci were conducted in parallel, using cells from the same donor (HSPCs), the same thawed batch (K562) and the same batch of prime editor mRNA along with freshly prepared sgRNA and pegRNA. These consistent experimental conditions suggest that the observed differences in editing efficiency are likely attributable to the genomic locus and cell type, highlighting the complexity and context-dependence of prime editing outcomes.

High expression of PE-GFP in samples targeting both *IL2RG* an *ARSA* in HSPCs as well as in K562 cells proves stability and efficient translation of mRNA after transfection. Therefore, the utilized prime editing mRNA is able to be expressed efficiently in both cell types.

A possible explanation for low editing efficiency when targeting *ARSA* P426L mutation could be the design of pegRNA. While in silico models can help predict the optimal pegRNA design for a specific target, these predictions do not always correlate with outcomes observed in in vitro or ex vivo experiments (Kim et al., 2021). For this reason, designing multiple pegRNAs and side by side comparison is important to find the most efficient pegRNA for a specific target sequence. However, testing multiple pegRNAs was not possible for this project.
Furthermore, a recent study by Nelson et al. showed that engineered pegRNAs (epegRNA), containing structured RNA motifs at the 3'-end, could increase prime editing efficiency up to 3- to 4-fold by preventing degradation of the 3'-end, which contains the RT template and the primer binding site (Nelson et al., 2022). With these things in mind, our pegRNA design could be further optimized to potentially achieve better editing efficiency.

Another possible explanation is that the genomic regions containing the two targeted mutations differ in their accessibility for the prime editing mechanism. It was shown that accessibility for genome editing can be limited by nucleosome configuration and heterochromatin in the genomic region (Kim et al., 2023). Furthermore, conversion of chromatin state from heterochromatin to euchromatin has been reported to improve prime editing efficiency (Liu et al., 2022). Since chromatin conformation and nucleosome organization are closely linked to gene expression levels (Kornberg & Lorch, 2020; Penagos-Puig & Furlan-Magaril, 2020), differences in editing efficiency between the *ARSA* P426L and *IL2RG* c.458T>C loci may be related to different expression levels of these genes in the transfected cell types. A study by Antony et al. showed that ARSA expression is significantly lower in HSPCs and K562 cells compared to fibroblasts and mesenchymal stromal cells (MSCs), indicating low expression in the cell types used in our experiments (Antony et al., 2022). In contrast, *IL2RG* expression has been reported in HSPCs and is thought to play a role in early hematopoiesis (Itano et al., 1996; Shultz et al., 2005), suggesting a higher level of transcriptional activity at this locus in HSPCs. More research about gene

expression patterns in target cells and site specific limitations for prime editing should be conducted to evaluate the importance of these factors when planning for prime editing experiments.

Another possible source for inefficiency of prime editing is the error frequency of the reverse transcriptase when transcribing repetitive sequences. These errors are more likely to occur with increasing length of the repetitive sequence (Kroutil et al., 1996). Furthermore, the reverse transcriptase incorporated in the prime editing mechanism, stemming from Moloney Murine Leukemia Virus (Anzalone et al., 2019), does not have exonucleolytic proofreading capabilities unlike most DNA-polymerases (Kroutil et al., 1996; Oscorbin & Filipenko, 2021). Even though the RT templates of our pegRNAs contained repetitive cytosine sequences of up to five in a row, sequencing data of the transfected cells did not show unwanted mutations in the target sequence.

Moreover, the choice of the prime editor can affect editing efficiency among different targets (Anzalone et al., 2019). There are further developed versions of prime editors that could be used to enhance editing efficiency. For instance, PE4 and PE5 utilize an additional inhibitor of the cells' innate DNA mismatch repair mechanism to prevent removal of the edited bases by the latter (Chen et al., 2021). Also, the architecture of the prime editing mechanism can be further optimized by introducing various structural modifications. These optimized prime editors, called PE2max, PE3max, PE4max and PE5max, significantly enhance editing efficiency compared to their non-optimized counterparts (Chen et al., 2021). These upgraded prime editors should be considered by researchers when struggling with low editing efficiency.

In the context of developing a prime editing based treatment for MLD, it remains uncertain how much ARSA expression must be restored in HSPCs to achieve a therapeutic effect following engraftment in the patient (Anzalone et al., 2019). This uncertainty is partly due to the complex and not yet fully understood mechanisms of action underlying allo-HSCT and Libmeldy (Wolf et al., 2020).

Based on current knowledge of allo-HSCT outcomes (Boucher et al., 2015), restoring at least physiological levels of ARSA expression is likely necessary to position prime editing as a competitive and effective therapeutic option for MLD (Antony et al., 2022).

4.4 Limitations of the study

Prime editing is a relatively new technology and has been subject of intensive research and constant evolution (Anzalone et al., 2022; Anzalone et al., 2019; Kantor et al., 2020). Testing different prime editors and pegRNAs to optimize our prime editing approach was not possible in this project. In addition, other factors like chromatin structure of the target region could potentially limit editing efficiency (Penagos-Puig & Furlan-Magaril, 2020). Therefore, information regarding the chromatin structure and transcription level of *ARSA* in K562 cells and HSPCs is needed to interpret the difference in editing efficiency for our two targeted mutations *ARSA* P426L and *IL2RG* c.458T>C.

Another limitation for this study was the availability of HSPCs. While K562 cells are a commercially available cell line, HSPCs had to be gathered from healthy donors. Available cell numbers for each donor were therefore limited in this study.

4.5 Conclusion

In conclusion, this study demonstrates that the *ARSA* P426L locus can, in principle, be targeted using prime editing, as shown by successful editing in K562 cells. Furthermore, the high editing efficiency achieved at the *IL2RG* c.458T>C locus in HSPCs confirms the general feasibility of prime editing mediated correction of disease-causing mutations in HSPCs, supporting its potential for therapeutic applications.

The contrary results observed for the two target loci in HSPCs highlight the importance of locus-specific factors, such as gene expression levels and chromatin structure, which should be considered when designing future editing strategies. Continued research in this area, along with the development of more advanced prime editing tools, may improve editing outcomes and expand the range of targetable mutations.

The implementation of a stem cell–based prime editing therapy for MLD will require sufficiently high editing efficiencies to ensure therapeutic efficacy, as well as a more comprehensive understanding of potential genotoxic effects associated with prime editing (Fiumara et al., 2023).

Taken together, this project provides valuable informations for the potential application of prime editing in stem cell–based gene therapies, including future treatments for disorders such as metachromatic leukodystrophy (MLD).

5. Summary

Metachromatic leukodystrophy (MLD) is a rare inherited lysosomal storage disease caused primarily by mutations in the *Arylsulfatase A* (*ARSA*) gene. Loss of functional ARSA leads to sulfatide accumulation, causing demyelination in the peripheral and central nervous system. MLD presents in different clinical forms, which all eventually result in severe neurological decline and death. Currently available treatment options are limited. Enzyme replacement therapy (ERT) and allogeneic hematopoietic stem cell transplantation (allo-HSCT) may slow disease progression but do not offer a cure. Libmeldy was recently approved by the European Medicines Agency (EMA) as the first gene therapy for early-onset forms of MLD. However, the potential long-term risk of insertional mutagenesis remains a concern and requires ongoing evaluation.

In this project we targeted the *ARSA* P426L mutation, one of the most common MLD-causing mutations in Europe. We used prime editing, a CRISPR-Cas9 based mechanism, which allows to introduce precise changes into the genome. The experiments were carried out in K562 cells and hematopoietic stem and progenitor cells (HSPCs). If the *ARSA* P426L mutation could be corrected ex vivo in patient-derived HSPCs prior to transplantation, this approach could offer a potentially curative treatment for patients who are currently lacking effective therapeutic options. Such a strategy would eliminate the need to find a matching donor for allogeneic HSCT, evade its side effects and avoid the risk of insertional mutagenesis associated with Libmeldy. Instead, it would restore physiological ARSA expression by precisely correcting the mutation at its endogenous locus.

In K562 cells, we successfully introduced the *ARSA* P426L mutation using prime editing, achieving mean editing efficiencies of 1.88% with PE2 and 10.20% with PE3. However, no editing was detected in HSPCs of healthy donors. As a result, this study did not progress to target patient-derived HSPCs. Further investigations are needed to focus on optimizing the prime editing mechanism as well as related components in order to achieve higher editing efficiency. Also research about target site specific limitations for prime editing should be closely monitored and taken into account when planning for future

projects. Although editing of the *ARSA* P426L locus was not successful, the high efficiency to induce the *IL2RG* c.458T>C mutation in HSPCs, which was used as a proof of concept, supports the general feasibility of prime editing based gene therapy approaches.

5.1 German summary

Metachromatische Leukodystrophie (MLD) ist eine seltene lysosomale Speicherkrankheit (LSK), die meist durch Mutationen im *Arylsulfatase-A* (*ARSA*) Gen verursacht wird. Der Verlust funktionellen ARSA-Enzyms führt zur Akkumulation von Sulfatiden im zentralen und peripheren Nervensystem, was wiederum zur Zerstörung der Markscheiden führt. Unterschiedliche klinische Verlaufsformen können unterschieden werden, jedoch gehen alle mit schweren neurologischen Symptomen einher und führen letztlich zum Tod.

Die aktuellen Behandlungsmöglichkeiten sind limitiert. Enzymersatztherapie (ERT) und die allogene Blutstammzelltransplantation (allo-HSZT) können das Fortschreiten der Krankheit verlangsamen, sind jedoch prinzipiell nicht kurativ. Libmeldy wurde kürzlich als erste Gentherapie zur Behandlung früh einsetzender Formen von MLD von der Europäischen Arzneimittelagentur (EMA) zugelassen. Das potenzielle Langzeitrisiko einer Libmeldy-assoziierten insertionalen Mutagenese erfordert jedoch weitere Langzeitstudien.

In diesem Projekt versuchten wir, die mit MLD assoziierte *ARSA* P426L Mutation in verschiedenen Zellreihen zu editieren. Dazu benutzten wir Prime Editing, einen CRISPR-Cas9-basierten Mechanismus, der präzise Veränderungen im Genom ermöglicht. Sollte es gelingen, die Mutation in HSPCs von erkrankten Patienten zu korrigieren und diese erfolgreich zurückzutransplantieren, wäre dies ein potenziell kurativer Therapieansatz für eine Patientengruppe, der aktuell keine effektive Therapie zur Verfügung steht. In diesem Fall könnten die aufwändige Spendersuche sowie die potenziell schwerwiegenden Nebenwirkungen einer allo-HSZT vermieden werden. Zudem gäbe es bei dieser Methode durch die präzise Korrektur des Gens keine Bedenken hinsichtlich insertionaler Mutagenese wie bei Libmeldy.

In K562-Zellen gelang es uns, die *ARSA* P426L Mutation erfolgreich zu induzieren. Die durchschnittliche Effizienz lag bei diesen Zellen bei 1.88% mit

PE2 und 10.20% mit PE3. In HSPCs gelang es leider nicht die Mutation zu induzieren. Ein Korrekturversuch mit HSPCs erkrankter Patienten fand aus diesem Grund nicht statt.

In zukünftigen Projekten sollte besonderer Wert darauf gelegt werden, Prime Editing und die dazugehörigen Komponenten zu optimieren, um bei der Editierung der Zielsequenz eine möglichst hohe Effizienz zu erreichen. Zudem sollten Daten bezüglich der Expression und Zugänglichkeit des entsprechenden Gens in unterschiedlichen Zellen gesammelt und in die Planung mit einbezogen werden.

Die gelungene effiziente Induzierung der *IL2RG* c.458T>C Mutation in HSPCs, welche als Positivkontrolle durchgeführt wurde, bietet hingegen eine gute Grundlage für weitere Forschung zu Prime Editing als Basis künftiger Gentherapien.

6. Bibliography

- Antony, J. S., Daniel-Moreno, A., Lamsfus-Calle, A., Raju, J., Kaftancioglu, M., Urena-Bailen, G., Rottenberger, J., Hou, Y., Santhanakumaran, V., Lee, J. H., Heumos, L., Bohringer, J., Krageloh-Mann, I., Handgretinger, R., & Mezger, M. (2022). A Mutation-Agnostic Hematopoietic Stem Cell Gene Therapy for Metachromatic Leukodystrophy. *CRISPR J*, *5*(1), 66-79. https://doi.org/10.1089/crispr.2021.0075
- Anzalone, A. V., Gao, X. D., Podracky, C. J., Nelson, A. T., Koblan, L. W., Raguram, A., Levy, J. M., Mercer, J. A. M., & Liu, D. R. (2022). Programmable deletion, replacement, integration and inversion of large DNA sequences with twin prime editing. *Nat Biotechnol*, *40*(5), 731-740. https://doi.org/10.1038/s41587-021-01133-w
- Anzalone, A. V., Randolph, P. B., Davis, J. R., Sousa, A. A., Koblan, L. W., Levy, J. M., Chen, P. J., Wilson, C., Newby, G. A., Raguram, A., & Liu, D. R. (2019). Search-and-replace genome editing without double-strand breaks or donor DNA. *Nature*, *576*(7785), 149-157. https://doi.org/10.1038/s41586-019-1711-4
- Beerepoot, S., Nierkens, S., Boelens, J. J., Lindemans, C., Bugiani, M., & Wolf, N. I. (2019). Peripheral neuropathy in metachromatic leukodystrophy: current status and future perspective. *Orphanet J Rare Dis*, *14*(1), 240. https://doi.org/10.1186/s13023-019-1220-4
- Beschle, J., Döring, M., Kehrer, C., Raabe, C., Bayha, U., Strölin, M., Böhringer, J., Bevot, A., Kaiser, N., Bender, B., Grimm, A., Lang, P., Müller, I., Krägeloh-Mann, I., & Groeschel, S. (2020). Early clinical course after hematopoietic stem cell transplantation in children with juvenile metachromatic leukodystrophy. *Mol Cell Pediatr*, *7*(1), 12. https://doi.org/10.1186/s40348-020-00103-7
- Biffi, A., Capotondo, A., Fasano, S., Carro, U. D., Marchesini, S., Azuma, H., Malaguti, M. C., Amadio, S., Brambilla, R., Grompe, M., Bordignon, C., Quattrini, A., & Naldini, L. (2006). Gene therapy of metachromatic leukodystrophy reverses neurological damage and deficits in mice. *Journal of Clinical Investigation*, *116*(11), 3070-3082. https://doi.org/10.1172/jci28873

- Biffi, A., De Palma, M., Quattrini, A., Del Carro, U., Amadio, S., Visigalli, I., Sessa, M., Fasano, S., Brambilla, R., Marchesini, S., Bordignon, C., & Naldini, L. (2004). Correction of metachromatic leukodystrophy in the mouse model by transplantation of genetically modified hematopoietic stem cells. *J Clin Invest*, *113*(8), 1118-1129. https://doi.org/10.1172/jci19205
- Boucher, A. A., Miller, W., Shanley, R., Ziegler, R., Lund, T., Raymond, G., & Orchard, P. J. (2015). Long-term outcomes after allogeneic hematopoietic stem cell transplantation for metachromatic leukodystrophy: the largest single-institution cohort report. *Orphanet J Rare Dis*, *10*, 94. https://doi.org/10.1186/s13023-015-0313-y
- Cesani, M., Lorioli, L., Grossi, S., Amico, G., Fumagalli, F., Spiga, I., Filocamo, M., & Biffi, A. (2016). Mutation Update ofARSAandPSAPGenes Causing Metachromatic Leukodystrophy. *Human Mutation*, *37*(1), 16-27. https://doi.org/10.1002/humu.22919
- Chen, P. J., Hussmann, J. A., Yan, J., Knipping, F., Ravisankar, P., Chen, P. F., Chen, C., Nelson, J. W., Newby, G. A., Sahin, M., Osborn, M. J., Weissman, J. S., Adamson, B., & Liu, D. R. (2021). Enhanced prime editing systems by manipulating cellular determinants of editing outcomes. *Cell*, *184*(22), 5635-5652.e5629. https://doi.org/10.1016/j.cell.2021.09.018
- Dalvie, N. C., Lorgeree, T., Biedermann, A. M., Love, K. R., & Love, J. C. (2022). Simplified Gene Knockout by CRISPR-Cas9-Induced Homologous Recombination. *ACS Synth Biol*, *11*(1), 497-501. https://doi.org/10.1021/acssynbio.1c00194
- Del Pozo-Rodríguez, A., Solinís, M., & Rodríguez-Gascón, A. (2016). Applications of lipid nanoparticles in gene therapy. *Eur J Pharm Biopharm*, *109*, 184-193. https://doi.org/10.1016/j.ejpb.2016.10.016
- Ejeskär, K., Fransson, S., Zaibak, F., & Ioannou, P. A. (2006). Method for efficient transfection of in vitro-transcribed mRNA into SK-N-AS and HEK293 cells: difference in the toxicity of nuclear EGFP compared to cytoplasmic EGFP. *Int J Mol Med*, *17*(6), 1011-1016.
- Fiumara, M., Ferrari, S., Omer-Javed, A., Beretta, S., Albano, L., Canarutto, D., Varesi, A., Gaddoni, C., Brombin, C., Cugnata, F., Zonari, E., Naldini, M.

M., Barcella, M., Gentner, B., Merelli, I., & Naldini, L. (2023). Genotoxic effects of base and prime editing in human hematopoietic stem cells. *Nature Biotechnology*. https://doi.org/10.1038/s41587-023-01915-4

- Fumagalli, F., Calbi, V., Natali Sora, M. G., Sessa, M., Baldoli, C., Rancoita, P. M. V., Ciotti, F., Sarzana, M., Fraschini, M., Zambon, A. A., Acquati, S., Redaelli, D., Attanasio, V., Miglietta, S., De Mattia, F., Barzaghi, F., Ferrua, F., Migliavacca, M., Tucci, F., . . . Aiuti, A. (2022). Lentiviral haematopoietic stem-cell gene therapy for early-onset metachromatic leukodystrophy: long-term results from a non-randomised, open-label, phase 1/2 trial and expanded access. *Lancet*, *399*(10322), 372-383. https://doi.org/10.1016/s0140-6736(21)02017-1
- Fumagalli, F., Zambon, A. A., Rancoita, P. M. V., Baldoli, C., Canale, S., Spiga, I., Medaglini, S., Penati, R., Facchini, M., Ciotti, F., Sarzana, M., Lorioli, L., Cesani, M., Natali Sora, M. G., Del Carro, U., Cugnata, F., Antonioli, G., Recupero, S., Calbi, V., . . . Sessa, M. (2021). Metachromatic leukodystrophy: A single-center longitudinal study of 45 patients. *Journal of Inherited Metabolic Disease*, *44*(5), 1151-1164. https://doi.org/10.1002/jimd.12388
- Groeschel, S., Kühl, J.-S., Bley, A. E., Kehrer, C., Weschke, B., Döring, M., Böhringer, J., Schrum, J., Santer, R., Kohlschütter, A., Krägeloh-Mann, I., & Müller, I. (2016). Long-term Outcome of Allogeneic Hematopoietic Stem Cell Transplantation in Patients With Juvenile Metachromatic Leukodystrophy Compared With Nontransplanted Control Patients. *JAMA Neurology*, *73*(9). https://doi.org/10.1001/jamaneurol.2016.2067
- Happi Mbakam, C., Rousseau, J., Tremblay, G., Yameogo, P., & Tremblay, J. P. (2022). Prime Editing Permits the Introduction of Specific Mutations in the Gene Responsible for Duchenne Muscular Dystrophy. *Int J Mol Sci*, *23*(11). https://doi.org/10.3390/ijms23116160
- Hou, Y., Ureña-Bailén, G., Mohammadian Gol, T., Gratz, P. G., Gratz, H. P., Roig-Merino, A., Antony, J. S., Lamsfus-Calle, A., Daniel-Moreno, A., Handgretinger, R., & Mezger, M. (2022). Challenges in Gene Therapy for Somatic Reverted Mosaicism in X-Linked Combined Immunodeficiency by

CRISPR/Cas9 and Prime Editing. *Genes (Basel)*, *13*(12). https://doi.org/10.3390/genes13122348

- Í Dali, C., Groeschel, S., Moldovan, M., Farah, M. H., Krägeloh-Mann, I., Wasilewski, M., Li, J., Barton, N., & Krarup, C. (2021). Intravenous arylsulfatase A in metachromatic leukodystrophy: a phase 1/2 study. *Ann Clin Transl Neurol*, *8*(1), 66-80. https://doi.org/10.1002/acn3.51254
- Í Dali, C., Sevin, C., Krägeloh-Mann, I., Giugliani, R., Sakai, N., Wu, J., & Wasilewski, M. (2020). Safety of intrathecal delivery of recombinant human arylsulfatase A in children with metachromatic leukodystrophy: Results from a phase 1/2 clinical trial. *Mol Genet Metab*, *131*(1-2), 235-244. https://doi.org/10.1016/j.ymgme.2020.07.002
- Ihry, R. J., Worringer, K. A., Salick, M. R., Frias, E., Ho, D., Theriault, K., Kommineni, S., Chen, J., Sondey, M., Ye, C., Randhawa, R., Kulkarni, T., Yang, Z., McAllister, G., Russ, C., Reece-Hoyes, J., Forrester, W., Hoffman, G. R., Dolmetsch, R., & Kaykas, A. (2018). p53 inhibits CRISPR-Cas9 engineering in human pluripotent stem cells. *Nat Med*, *24*(7), 939-946. https://doi.org/10.1038/s41591-018-0050-6
- Itano, M., Tsuchiya, S., Morita, S., Fujie, H., Ishii, N., Yanagisawa, T., Ohashi, Y., Minegishi, M., Sugamura, K., & Konno, T. (1996). IL-2 receptor gamma chain expression on CD34 positive hematopoietic progenitor cells from bone marrow and cord blood. *Tohoku J Exp Med*, *178*(4), 389-398. https://doi.org/10.1620/tjem.178.389
- Jeyakumar, M., Smith, D. A., Williams, I. M., Borja, M. C., Neville, D. C., Butters, T. D., Dwek, R. A., & Platt, F. M. (2004). NSAIDs increase survival in the Sandhoff disease mouse: synergy with N-butyldeoxynojirimycin. *Ann Neurol*, *56*(5), 642-649. https://doi.org/10.1002/ana.20242
- Jinek, M., Chylinski, K., Fonfara, I., Hauer, M., Doudna, J. A., & Charpentier, E. (2012). A programmable dual-RNA-guided DNA endonuclease in adaptive bacterial immunity. *Science*, *337*(6096), 816-821. https://doi.org/10.1126/science.1225829

- Jonckheere, A. I., Kingma, S. D. K., Eyskens, F., Bordon, V., & Jansen, A. C. (2023). Metachromatic leukodystrophy: To screen or not to screen? *Eur J Paediatr Neurol*, *46*, 1-7. https://doi.org/10.1016/j.ejpn.2023.06.005
- Kantor, A., McClements, M., & Maclaren, R. (2020). CRISPR-Cas9 DNA Base-Editing and Prime-Editing. *International Journal of Molecular Sciences*, *21*(17), 6240. https://doi.org/10.3390/ijms21176240
- Kim, H. K., Yu, G., Park, J., Min, S., Lee, S., Yoon, S., & Kim, H. H. (2021). Predicting the efficiency of prime editing guide RNAs in human cells. *Nat Biotechnol*, *39*(2), 198-206. https://doi.org/10.1038/s41587-020-0677-y
- Kim, S., Yuan, J. B., Woods, W. S., Newton, D. A., Perez-Pinera, P., & Song, J. S. (2023). Chromatin structure and context-dependent sequence features control prime editing efficiency. *bioRxiv*. https://doi.org/10.1101/2023.04.15.536944
- Kontomanolis, E. N., Koutras, A., Syllaios, A., Schizas, D., Mastoraki, A., Garmpis, N., Diakosavvas, M., Angelou, K., Tsatsaris, G., Pagkalos, A., Ntounis, T., & Fasoulakis, Z. (2020). Role of Oncogenes and Tumor-suppressor Genes in Carcinogenesis: A Review. *Anticancer Res*, *40*(11), 6009-6015. https://doi.org/10.21873/anticanres.14622
- Kornberg, R. D., & Lorch, Y. (2020). Primary Role of the Nucleosome. *Mol Cell*, *79*(3), 371-375. https://doi.org/10.1016/j.molcel.2020.07.020
- Krägeloh-Mann, I., & Groeschel, S. (2016). Therapies of lysosomal storage disorders targeting the brain. *The Lancet*, *388*(10043), 440-442. https://doi.org/10.1016/s0140-6736(16)30450-0
- Kroutil, L. C., Register, K., Bebenek, K., & Kunkel, T. A. (1996). Exonucleolytic proofreading during replication of repetitive DNA. *Biochemistry*, *35*(3), 1046-1053. https://doi.org/10.1021/bi952178h
- Levesque, S. B., D. E.;. (2023). Modulating Nucleotide Metabolism Enhances Prime Editing in Hematopoietic Stem and Progenitor Cells. *Blood Adv*, *142*(2 November 2023), 7124. https://doi.org/https://doi.org/10.1182/blood-2023-190750
- Li, C., Liu, Z., Anderson, J., Liu, Z., Tang, L., Li, Y., Peng, N., Chen, J., Liu, X., Fu, L., Townes, T. M., Rowe, S. M., Bedwell, D. M., Guimbellot, J., & Zhao, R.

(2023). Prime editing-mediated correction of the CFTR W1282X mutation in iPSCs and derived airway epithelial cells. *PLoS One*, *18*(11), e0295009. https://doi.org/10.1371/journal.pone.0295009

- Li, J., Sun, H., Huang, Y., Wang, Y., Liu, Y., & Chen, X. (2019). Pathways and assays for DNA double-strand break repair by homologous recombination. *Acta Biochim Biophys Sin (Shanghai)*, *51*(9), 879-889. https://doi.org/10.1093/abbs/gmz076
- Liu, N., Zhou, L., Lin, G., Hu, Y., Jiao, Y., Wang, Y., Liu, J., Yang, S., & Yao, S. (2022). HDAC inhibitors improve CRISPR-Cas9 mediated prime editing and base editing. *Mol Ther Nucleic Acids*, *29*, 36-46. https://doi.org/10.1016/j.omtn.2022.05.036
- Lugowska, A., Amaral, O., Berger, J., Berna, L., Bosshard, N. U., Chabas, A., Fensom, A., Gieselmann, V., Gorovenko, N. G., Lissens, W., Mansson, J. E., Marcao, A., Michelakakis, H., Bernheimer, H., Ol'khovych, N. V., Regis, S., Sinke, R., Tylki-Szymanska, A., & Czartoryska, B. (2005). Mutations c.459+1G>A and p.P426L in the ARSA gene: prevalence in metachromatic leukodystrophy patients from European countries. *Mol Genet Metab*, *86*(3), 353-359. https://doi.org/10.1016/j.ymgme.2005.07.010
- Luzi, P., Abraham, R. M., Rafi, M. A., Curtis, M., Hooper, D. C., & Wenger, D. A. (2009). Effects of treatments on inflammatory and apoptotic markers in the CNS of mice with globoid cell leukodystrophy. *Brain Res*, *1300*, 146-158. https://doi.org/10.1016/j.brainres.2009.09.017
- Matthes, F., Stroobants, S., Gerlach, D., Wohlenberg, C., Wessig, C., Fogh, J., Gieselmann, V., Eckhardt, M., D'Hooge, R., & Matzner, U. (2012). Efficacy of enzyme replacement therapy in an aggravated mouse model of metachromatic leukodystrophy declines with age. *Hum Mol Genet*, *21*(11), 2599-2609. https://doi.org/10.1093/hmg/dds086
- Matzner, U., Hartmann, D., Lüllmann-Rauch, R., Coenen, R., Rothert, F., Månsson, J. E., Fredman, P., D'Hooge, R., De Deyn, P. P., & Gieselmann, V. (2002). Bone marrow stem cell-based gene transfer in a mouse model for metachromatic leukodystrophy: effects on visceral and nervous system

disease manifestations. *Gene Ther*, *9*(1), 53-63. https://doi.org/10.1038/sj.gt.3301593

- Matzner, U., Lüllmann-Rauch, R., Stroobants, S., Andersson, C., Weigelt, C., Eistrup, C., Fogh, J., D'Hooge, R., & Gieselmann, V. (2009). Enzyme Replacement Improves Ataxic Gait and Central Nervous System Histopathology in a Mouse Model of Metachromatic Leukodystrophy. *Molecular Therapy*, *17*(4), 600-606. https://doi.org/10.1038/mt.2008.305
- Messina, M., & Gissen, P. (2023). Atidarsagene autotemcel for metachromatic leukodystrophy. *Drugs of Today*, *59*(2), 63-70. https://doi.org/10.1358/dot.2023.59.2.3461911
- Mollanoori, H., & Teimourian, S. (2018). Therapeutic applications of CRISPR/Cas9 system in gene therapy. *Biotechnol Lett*, *40*(6), 907-914. https://doi.org/10.1007/s10529-018-2555-y
- Muschol, N., Matzner, U., Tiede, S., Gieselmann, V., Ullrich, K., & Braulke, T. (2002). Secretion of phosphomannosyl-deficient arylsulphatase A and cathepsin D from isolated human macrophages. *Biochemical Journal*, *368*(3), 845-853. https://doi.org/10.1042/bj20020249
- Nelson, J. W., Randolph, P. B., Shen, S. P., Everette, K. A., Chen, P. J., Anzalone, A. V., An, M., Newby, G. A., Chen, J. C., Hsu, A., & Liu, D. R. (2022). Engineered pegRNAs improve prime editing efficiency. *Nat Biotechnol*, *40*(3), 402-410. https://doi.org/10.1038/s41587-021-01039-7
- Oscorbin, I. P., & Filipenko, M. L. (2021). M-MuLV reverse transcriptase: Selected properties and improved mutants. *Comput Struct Biotechnol J*, *19*, 6315-6327. https://doi.org/10.1016/j.csbj.2021.11.030
- Penagos-Puig, A., & Furlan-Magaril, M. (2020). Heterochromatin as an Important Driver of Genome Organization. *Front Cell Dev Biol*, *8*, 579137. https://doi.org/10.3389/fcell.2020.579137
- Peters, C., & Steward, C. G. (2003). Hematopoietic cell transplantation for inherited metabolic diseases: an overview of outcomes and practice guidelines. *Bone Marrow Transplant*, *31*(4), 229-239. https://doi.org/10.1038/sj.bmt.1703839

- Rauschka, H., Colsch, B., Baumann, N., Wevers, R., Schmidbauer, M., Krammer, M., Turpin, J. C., Lefevre, M., Olivier, C., Tardieu, S., Krivit, W., Moser, H., Moser, A., Gieselmann, V., Zalc, B., Cox, T., Reuner, U., Tylki-Szymanska, A., Aboul-Enein, F., . . . Berger, J. (2006). Late-onset metachromatic leukodystrophy: genotype strongly influences phenotype. *Neurology*, *67*(5), 859-863. https://doi.org/10.1212/01.wnl.0000234129.97727.4d
- Schene, I. F., Joore, I. P., Oka, R., Mokry, M., van Vugt, A. H. M., van Boxtel, R., van der Doef, H. P. J., van der Laan, L. J. W., Verstegen, M. M. A., van Hasselt, P. M., Nieuwenhuis, E. E. S., & Fuchs, S. A. (2020). Prime editing for functional repair in patient-derived disease models. *Nat Commun*, *11*(1), 5352. https://doi.org/10.1038/s41467-020-19136-7
- Shultz, L. D., Lyons, B. L., Burzenski, L. M., Gott, B., Chen, X., Chaleff, S., Kotb, M., Gillies, S. D., King, M., Mangada, J., Greiner, D. L., & Handgretinger, R. (2005). Human lymphoid and myeloid cell development in NOD/LtSz-scid IL2R gamma null mice engrafted with mobilized human hemopoietic stem cells. *J Immunol*, *174*(10), 6477-6489. https://doi.org/10.4049/jimmunol.174.10.6477
- Smith, D., Wallom, K. L., Williams, I. M., Jeyakumar, M., & Platt, F. M. (2009). Beneficial effects of anti-inflammatory therapy in a mouse model of Niemann-Pick disease type C1. *Neurobiol Dis*, *36*(2), 242-251. https://doi.org/10.1016/j.nbd.2009.07.010
- Stroobants, S., Gerlach, D., Matthes, F., Hartmann, D., Fogh, J., Gieselmann, V., D'Hooge, R., & Matzner, U. (2011). Intracerebroventricular enzyme infusion corrects central nervous system pathology and dysfunction in a mouse model of metachromatic leukodystrophy. *Human Molecular Genetics*, *20*(14), 2760-2769. https://doi.org/10.1093/hmg/ddr175
- Ureña-Bailén, G., Dobrowolski, J. M., Hou, Y., Dirlam, A., Roig-Merino, A., Schleicher, S., Atar, D., Seitz, C., Feucht, J., Antony, J. S., Mohammadian Gol, T., Handgretinger, R., & Mezger, M. (2022). Preclinical Evaluation of CRISPR-Edited CAR-NK-92 Cells for Off-the-Shelf Treatment of AML and B-ALL. *Int J Mol Sci*, *23*(21). https://doi.org/10.3390/ijms232112828

- van den Broek, B. T. A., Page, K., Paviglianiti, A., Hol, J., Allewelt, H., Volt, F., Michel, G., Diaz, M. A., Bordon, V., O'Brien, T., Shaw, P. J., Kenzey, C., Al-Seraihy, A., van Hasselt, P. M., Gennery, A. R., Gluckman, E., Rocha, V., Ruggeri, A., Kurtzberg, J., & Boelens, J. J. (2018). Early and late outcomes after cord blood transplantation for pediatric patients with inherited leukodystrophies. *Blood Adv*, *2*(1), 49-60. https://doi.org/10.1182/bloodadvances.2017010645
- van Rappard, D. F., Boelens, J. J., van Egmond, M. E., Kuball, J., van Hasselt, P. M., Oostrom, K. J., Pouwels, P. J. W., van der Knaap, M. S., Hollak, C. E. M., & Wolf, N. I. (2016). Efficacy of hematopoietic cell transplantation in metachromatic leukodystrophy: the Dutch experience. *Blood Adv*, *127*(24), 3098-3101. https://doi.org/10.1182/blood-2016-03-708479
- van Rappard, D. F., Boelens, J. J., & Wolf, N. I. (2015). Metachromatic leukodystrophy: Disease spectrum and approaches for treatment. *Best Pract Res Clin Endocrinol Metab*, *29*(2), 261-273. https://doi.org/10.1016/j.beem.2014.10.001
- Videbæk, C., Stokholm, J., Sengeløv, H., Fjeldborg, L. U., Larsen, V. A., Krarup, C., Nielsen, J. E., & Grønborg, S. (2021). Allogenic hematopoietic stem cell transplantation in two siblings with adult metachromatic leukodystrophy and a systematic literature review. *JIMD Rep*, *60*(1), 96-104. https://doi.org/10.1002/jmd2.12221
- Wilfinger, W. W., Mackey, K., & Chomczynski, P. (1997). Effect of pH and ionic strength on the spectrophotometric assessment of nucleic acid purity. *Biotechniques*, *22*(3), 474-476, 478-481. https://doi.org/10.2144/97223st01
- Wolf, N. I., Breur, M., Plug, B., Beerepoot, S., Westerveld, A. S. R., van Rappard, D. F., de Vries, S. I., Kole, M. H. P., Vanderver, A., van der Knaap, M. S., Lindemans, C. A., van Hasselt, P. M., Boelens, J. J., Matzner, U., Gieselmann, V., & Bugiani, M. (2020). Metachromatic leukodystrophy and transplantation: remyelination, no cross-correction. *Ann Clin Transl Neurol*, *7*(2), 169-180. https://doi.org/10.1002/acn3.50975
- Zhao, Y., Zheng, Z., Cohen, C. J., Gattinoni, L., Palmer, D. C., Restifo, N. P., Rosenberg, S. A., & Morgan, R. A. (2006). High-efficiency transfection of

primary human and mouse T lymphocytes using RNA electroporation. *Mol Ther*, *13*(1), 151-159. https://doi.org/10.1016/j.ymthe.2005.07.688

7. Appendix

A1: Figure 3 (Plasmid map for PE2 & PE2-GFP)

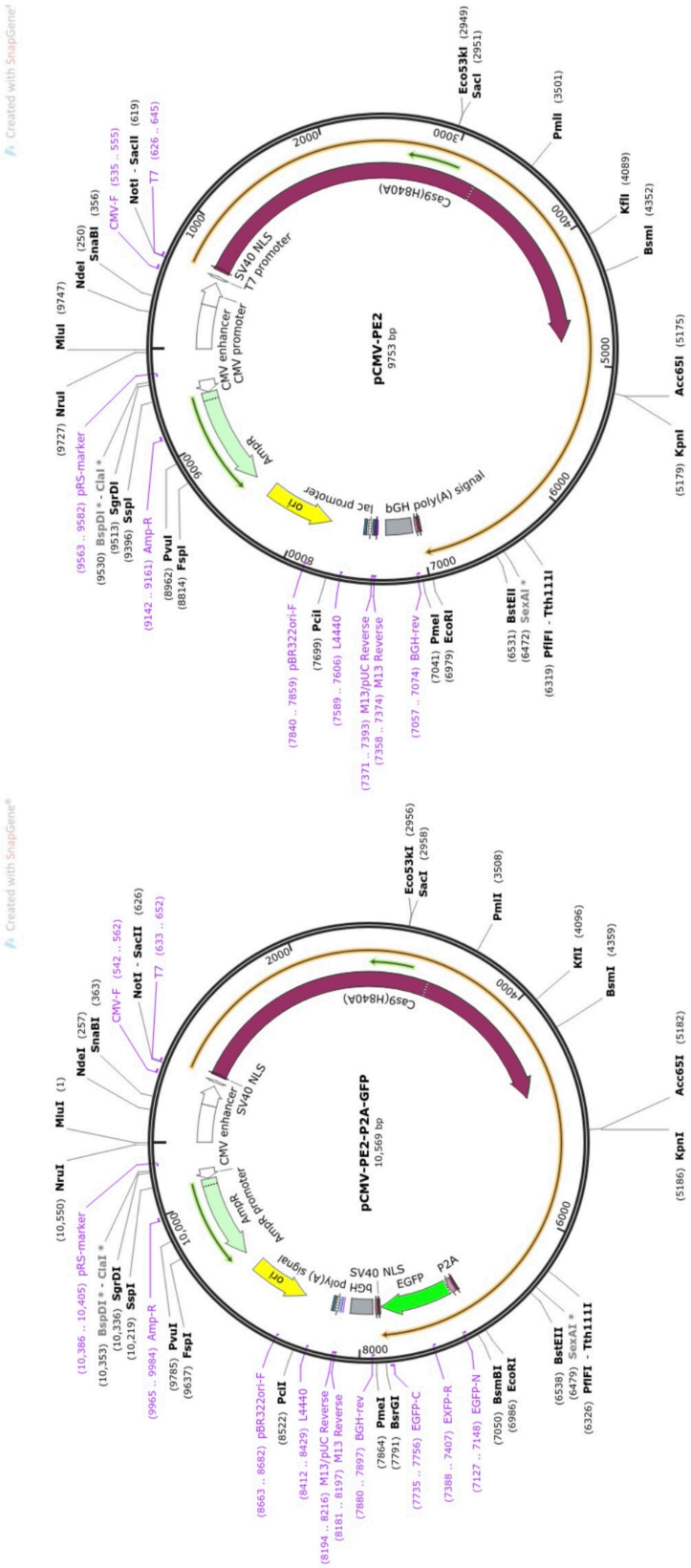

8. Declaration of own Contribution

This project was carried out under the supervision of PD Dr. med. Dr. rer. nat. Dipl. Biol. Markus Mezger in the laboratory for Hematology & Oncology, belonging to the Department for Pediatrics of the University Hospital Tübingen.

The concept of this study was designed by PD Dr. med. Dr. rer. nat. Dipl. Biol. Markus Mezger as the head of the research group and Dr. Tahereh Mohammadian Gol.
All the experiments were carried out independently by me after getting introduced to the techniques by members of our group: Yujuan Hou (MD PhD student), Dr. Tahereh Mohammadian Gol (postdoctoral researcher) and Guillermo Ureña Bailén (PhD student).
Established techniques were optimized by me throughout the course of the project.
The results were analyzed by myself and discussed with PD Dr. med. Dr. rer. nat. Dipl. Biol. Markus Mezger, Dr. Tahereh Mohammadian Gol and Guillermo Ureña Bailén.

Consensus (AI Search Engine for Research) was used for literature research when conventional database screening was exhausted. Content of papers was thoroughly verified in every case. AI-based language tools (e.g., ChatGPT) were occasionally used to improve the structure of selected passages. All intellectual content, analysis, and conclusions are my own.

I hereby declare that this dissertation was done by myself, all the presented data resulted from my own work and that I didn't use any other sources than the ones cited in this manuscript.

Tübingen 07.01.2026 Paul Luis Trosien

_____

Place date signature of doctoral candidate

9. Publications

- Gene therapy in pediatrics - Clinical studies and approved drugs (as of 2023) (Mohammadian Gol, T., Zahedipour, F., Trosien, P., Ureña-Bailén, G., Kim, M., Antony, J. S., & Mezger, M. (2024). Gene therapy in Pediatrics – Clinical Studies and approved drugs (as of 2023). *Life Sciences*, *348*, 122685. https://doi.org/10.1016/j.lfs.2024.122685)

10. Acknowledgements

First of all, I want to thank PD Dr. med. Dr. rer. nat. Dipl. Biol. Markus Mezger for his continuous professional and personal support throughout the course of this thesis. Without his dedication to research in the field of medicine, this project could have never happened in the first place.

I would also like to thank Dr. Tahereh Mohammadian Gol and Dr. Guillermo Ureña Bailén for their professional and emotional support during the course of this project.

Furthermore I like to thank all other members of AG Mezger and other research groups in our lab (Dr. Yujuan Hou, Miso Kim, Ralph Sinn, Derya Güngör, Stella Halacheva, Ina Becoku, Aylin Kuru, Daniel Stowitschek, Fatemeh Zahedipour, Moustafa Moustafa-Oglou and many more) who brightened the sun-deprived lab-days during the time of my studies.

Apart from that, I would like to give a special thanks to my friends and family as well as my girlfriend Christina. Thank you for always cheering me up, supporting me through the struggles as well as celebrating the good times with me. I can not imagine where I would be without you as my supporting cast!

Writing this, I feel incredibly blessed for all the wonderful people that I met on this journey. Thank you for everything!